Electrochimica Acta 439 (2023) 141678

Contents lists available at ScienceDirect

Electrochimica Acta

journal homepage: www.journals.elsevier.com/electrochimica-acta

Mesoporous carbon-based materials and their applications as non-precious metal electrocatalysts in the oxygen reduction reaction

Gillian Collins [a,1], Palanisamy Rupa Kasturi [a,1], Raj Karthik [b,1], Jae-Jin Shim [b,1], Ramaraj Sukanya [a,1,*], Carmel B. Breslin [a,c,1,*]

[a] Department of Chemistry, Maynooth University, Maynooth, Co. Kildare, Ireland
[b] School of Chemical Engineering, Yeungnam University, Gyeongsan, Gyeongbuk 38541, Republic of Korea
[c] Kathleen Lonsdale Institute, Maynooth University, Maynooth, Co. Kildare, Ireland

ARTICLE INFO

Keywords:
Mesoporous carbon
Oxygen reduction reaction
Hydrogen peroxide
Heteroatom doping
Electrocatalysts
Single atom electrocatalysts
M-N-C catalysts
Non-precious metal catalysts

ABSTRACT

Carbon is truly astonishing and the only element that can form so many different compounds and materials. In recent years, numerous nanostructured carbon-based materials have emerged and within this family, mesoporous and ordered mesoporous carbon have attracted considerable attention. In this paper, we review the recent developments in the applications of mesoporous carbon as an electrocatalyst for the oxygen reduction reaction (ORR). The ORR is one of the most studied electrochemical reactions with applications in the energy and environmental sectors. Following a short introduction to the methodologies employed in the fabrication of mesoporous and ordered mesoporous carbon, the performance of these materials in the ORR is reviewed. Initially, metal free heteroatom doped mesoporous carbon electrocatalysts are described, highlighting the roles of N, S and B as dopants. Next, mesoporous carbon materials with Fe, Co, Mn and Ni, as isolated single atom catalysts, are introduced. The role of mesoporous carbon as a support for nanostructured electrocatalysts is then discussed. Finally, the selectivity of the mesoporous carbon-based electrocatalysts for the four and two-electron ORR is discussed.

While further developments and advancements are needed, it is clear that these mesoporous carbon-based materials have the potential to give highly efficient electrocatalysts for both the four and two electron ORR. Indeed, many of the reported electrocatalysts can outperform the commercial Pt/carbon electrocatalysts in alkaline solutions.

1. General introduction

Carbon is a truly remarkable element and continues to deliver a host of new, interesting, and fascinating materials. Its unique ability to form a multitude of diverse nanostructures has led to the development of fullerenes [1,2], carbon nanotubes [2,3], including single and multi-walled carbon nanotubes, graphene [2], graphene oxide, reduced graphene oxide [4] and graphene quantum dots [5], carbon fibres [6] and various porous carbon-based materials [7,8]. These carbon based materials have been used in a myriad of applications, extending from medical [9], electrochemical sensors and biosensors [10], energy conversion and storage [11] to adsorbents for the treatment of wastewater [12]. Family members such as mesoporous carbon (MC) and the more recently discovered ordered mesoporous carbon (OMC), which was first reported in 1999 [13,14], are now attracting considerable interest. The porosity of carbon materials is normally classified depending on IUPAC definitions, with pore diameters less than 2 nm giving micro porosity, while diameters between 2 and 50 nm are considered as mesoporous, and macroporous carbon has pore diameters greater than 50 nm. Therefore, MC and OMC have pore diameters typically between 2 and 50 nm.

Traditional porous carbon materials have a long history and have been used successfully in different applications, ranging from adsorbents for environmental pollutants, in filtration, energy storage and as support materials for electrocatalysts, with numerous applications in electrochemistry [15–17]. This is not surprising as these materials have large surface areas, excellent thermal and mechanical stability, high electrical conductivity and can be synthesised from readily available precursors, making them cost-effective. However, in recent years, there has been a

* Corresponding authors at: Department of Chemistry, Maynooth University, Maynooth, Co. Kildare, Ireland.
E-mail addresses: sukanyaram33@gmail.com (R. Sukanya), Carmel.Breslin@mu.ie (C.B. Breslin).
[1] These authors contributed equally to this work.

https://doi.org/10.1016/j.electacta.2022.141678
Received 26 August 2022; Received in revised form 1 December 2022; Accepted 3 December 2022
Available online 5 December 2022

clear and increasing focus on mesoporous carbons, including MC and OMC [18–20]. Mesoporous carbon is particularly interesting from an electrochemical viewpoint, as the pore size is sufficiently small to give a very high surface area, but also suitably large for the diffusion of molecules and electrolyte ions. On the other hand, the micropores are too small for the transport of electrolyte ions and molecules, while the macroporous carbon has a lower surface area. MC and OMC are related in terms of pore sizes, with OMC having a well ordered and uniform assembly and network of mesopores. These mesoporous materials have good stability, high specific surface areas, controllable pore structures coupled with low cost, and are attracting interest in chemistry, physics, material science, membrane science, catalysis, analytical chemistry and especially electrochemistry [21–23].

Mesoporous carbon has also been modified to generate hierarchical porous materials, which are formed by interlinking macro- and mesoporous structures [24,25]. This strategy has been used to enhance diffusion and mass transport. Likewise, the electrochemical and electrocatalytic activity can be enhanced through the doping of MC with elements such as sulfur or nitrogen [26,27]. These electron rich heteroatoms can alter the electronic and physicochemical properties of the OMC/MC, increasing its electrochemical properties, with higher rates of charge transfer, and enhanced specific capacitance and stability. Interestingly, it has also been shown that the incorporation of very low concentrations of transition metals, typically between 0.05 and 1.05 wt %, can increase the electrocatalytic performance of the OMC [28,29]. In addition, MC has been employed frequently as a support for electrocatalysts such as metal nanoparticles [30].

In summary, the MC and OMC families of carbon-based materials are interesting with a bright future in electrochemistry and energy-based applications. It is possible to tune their properties by altering their surface area, size of the mesopores, or by the introduction of macropores, heteroatoms, single atom transition metals, and decoration with various nanoparticles or nanostructures. In particular, these materials have the potential to serve as electrocatalysts for the oxygen reduction reaction (ORR), and therefore have the potential to contribute to renewable energy and offer solutions to address and reduce the impact of climate change [31]. The ORR is not only an important reaction in biochemical processes, but also a central half reaction in energy conversion systems, such as fuel cells and metal-air batteries. For these applications, the four-electron transfer reaction that converts oxygen into water is the favoured reduction reaction. Nevertheless, the two electron transfer half reaction, which is often described as the less efficient, leads to the formation of hydrogen peroxide, and this is very relevant in the production of hydrogen peroxide and the related electro-Fenton, and photo-electro-Fenton technologies [32]. These Fenton technologies, which are based on the reaction of hydrogen peroxide with ferrous ions, are important in the removal of contaminants and pollutants from aquatic environments [33,34]. Therefore, the recent developments in the fabrication of MC and OMC with tailored pore sizes and networks coupled with high conductivity are timely, making these materials interesting in both energy and environmental sectors.

In this review, the recent developments in the application of MC and OMC-based ORR electrocatalysts are introduced and discussed. Initially, the methods typically employed in the fabrication of MC and OMC are reviewed, followed by a short introduction to the ORR. The remainder of the review is devoted to the applications of MC and OMC-based electrocatalysts in catalysing and facilitating the ORR, with a focus on heteroatom doping, atomic transition metals and MC as an immobilisation matrix for nanostructures. Finally, the selectivity of the ORR reaction is reviewed to delve into the characteristics required to favour the two and four electron transfer reactions.

2. A brief introduction to the formation of mesoporous and ordered mesoporous carbon

There has been significant advances in the synthesis of MC and OMC, especially over the last two decades. A number of excellent reviews on the various synthetic methods that can be employed to give both MC and OMC are already available [35,36]. For example, Vinu and co-workers [36] reviewed the synthesis and applications of functionalised micro and mesoporous carbon materials, Eftekhari and Fan reviewed OMC and its applications in energy storage [21], while in an earlier review Liang et al. [37] provided a detailed account of the synthetic methods together with a historical outline of the major developments in the synthesis of OMC. Therefore, in this section a brief summary of some of the synthetic methods employed to give MC and OMC is provided, while more detailed reviews on the synthesis of these mesoporous materials are already available in the recent literature [21,35–37].

OMC is normally formed using either hard- or soft-templating methods. In the hard templating process, the template, which is generally ordered mesoporous templated silica, is employed as a mould to give OMC with an inverse pore structure of the silica template. Typically, the silica pores in the ordered mesoporous silica are impregnated with the carbon precursors and then subjected to a carbonisation routine at high temperatures, as evident in Fig. 1(a). Using acidic or alkaline etching conditions, the silica template can be removed, with the volume once occupied by the silica becoming the mesopores within the carbon, giving rise to OMC. This methodology depends strongly on the interconnected porous structure of the template. Various templates have been employed with the first template used in 1999 being MCM-48 mesoporous silica [13]. Since then hard templates based on silica and zeolites have been employed, such as the ordered SBA-15 silica [38,39], core/shell type aluminosilicates [40] and hexagonal mesoporous aluminosilicate (Al-HMS) [41]. More recently, HZSM-5/SBA-15 micro-mesoporous templates have been used to give ordered micro-mesoporous carbon [42]. The silica-based templates have a highly ordered mesoporous architecture and this is a key advantage in the formation of OMC using hard templates. Nevertheless, the acidic treatments required to remove the silica-based templates are aggressive and these not only have negative environmental impact but can also modify the OMC. Environmentally acceptable and sustainable alternatives have been employed and these include the use of iron and magnesium based nanoparticles/nanostructures as templates. Indeed it was shown by Niu et al. [43] that FeO(OH) nanorods distributed homogeneously within the polymer matrix can serve as rigid templates. These nanorods were subsequently removed thermally through the decomposition of the FeO(OH) nanorods at elevated temperatures to yield the formation of MC. Iron oxide nanoparticles [44], sheet-like magnesium hydroxide [45] and MgO [46] have also been employed as templates, as these are easily removed using dilute acids.

Recently, there has been more focus on the formation of mesoporous materials including carbon with soft-templating or self-templating strategies. The removal of silica-based hard templates requires acidic conditions that necessitates the use of HF, which is both toxic and corrosive, while the alkaline methods require high concentrations of hydroxides. As the soft-templating method does not require the removal of the hard template, it is considered to be a convenient scalable, more environmentally acceptable and cost-effective strategy. In the soft templating approaches, it is possible to synthesise the OMC by the self-assembly of the carbon precursors and surfactant copolymers. In this case the surfactant template is removed during the pyrolysis step in the formation of the OMC structures. The size of the pores within OMC are dictated by the chemical nature and ratio of the copolymer and the organic precursors, and the weak interactions, such as hydrogen bonding, between them. Various OMCs have been formed using this approach and one of the more popular strategies is derived from the classical solvent evaporation induced self-assembly methodology [25, 47–52]. For example, Meng et al. [48] synthesised a family of OMC

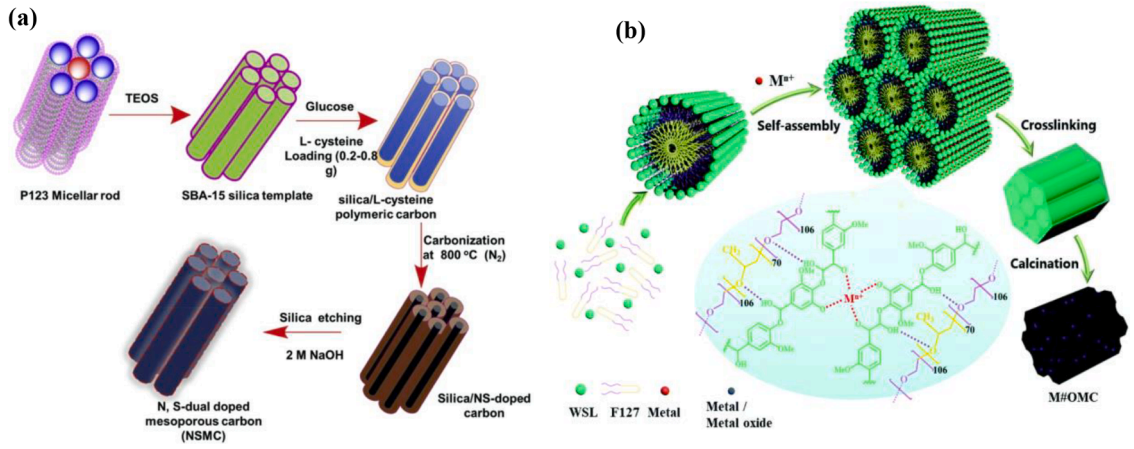

Fig. 1. Synthesis protocol for OMCs using **(a)** N, S dual doped OMC with the hard SBA-15 silica template, reprinted with permission from Elsevier and taken from Duraisamy et al. [38], and **(b)** evaporation-induced self-assembly (EISA) with a soft template and calcination, using lignin (WSL) as the carbon precursor, F127 as a surfactant, and the metal ion crosslinker, reproduced with permission from the Royal Society of Chemistry and taken from Wang et al. [58].

structures from the assembly of organic-organic triblock copolymers with soluble phenolic precursors by the evaporation induced self-assembly process. By simply adjusting the ratios of phenol to the copolymer, OMC with two-dimensional hexagonal (p6m space group), body-centred cubic (Im3m), three-dimensional bi-continuous (Ia3d), or lamellar OMC were formed. Hydrothermal synthesis has also been employed in the fabrication of OMC structures, where all the precursors are mixed and then transferred to a Teflon-lined autoclave and heated for several hours at relatively low temperatures [53–57]. This is then followed by carbonisation to give the OMC structures.

Although the soft templating protocols are attractive, they rely mainly on the use of phenolic based carbon precursors with aldehyde cross-linkers that are not always environmentally acceptable. Therefore, much of the recent focus is devoted to the fabrication of OMC materials using sustainable and environmentally acceptable precursors. The classical solvent evaporation induced self-assembly methodology has recently been employed to synthesise OMC using a green and sustainable strategy, where natural biopolymers, such as lignin are used. For example, Wang et al. [58] combined lignin extracted from walnut shells, Pluronic F127 as the surfactant, acetone as a solvent, and a nickel salt as the crosslinking agent. The solvent was then evaporated followed by heating at 100 °C to induce further cross-linking and polymerisation before the final calcination and carbonisation steps were applied. This process resulted in the formation of 2D hexagonal ordered mesopores, as illustrated in Fig. 1(b), with diameters varying from 4.4 to 13.0 nm depending on the calcination temperature and metal ion (nickel) concentrations. Other commonly used cross-linking ions are Fe(III) [59].

In terms of electrochemical applications, it is well established that the degree of graphitisation has a significant effect on the electrical conductivity of MC and OMC. An increase in the electrochemical properties, such as capacitance and cyclic stability, is observed on enhancing the level of graphitisation and this is normally achieved using post-synthetic thermal treatments at temperatures greater than 2000 °C [60,61]. Nevertheless, these high temperatures can give rise to the collapse of the ordered mesoporous structure and reduce the surface area, limiting the potential applications of OMC when high surface area, porosity and electrical conductivity are all equally critical. However, it has been shown that the graphitisation temperature depends on the nature of the carbon precursors, with polyaromatic or aromatic carbon-based precursors normally requiring lower graphitisation temperatures [62]. Indeed OMCs with graphitic character have been formed using carbon precursors such as phenanthrene at a temperature in the vicinity of 1075 °C [63], acenaphthene with thermal treatment at 900 °C [62], and naphthalene at 750 °C, anthracene at 800 °C and pyrene at 850 °C [64]. In addition, various metal catalysts, such as Ni [65,66] and Fe [67–70] have been used during the synthetic process to create graphitic domains (catalytic graphitisation) at lower temperatures. For example, Sevilla and Fuertes [71] used a two-step process, where the MC was first synthesised using mesoporous silica xerogel as the template. The prepared porous carbon was then impregnated with Fe, Ni or Mn and heated to 900 °C to induce graphitisation.

Traditional porous-carbon-based electrocatalysts are limited by diffusion of the ions within the pores, which can be complex due to the size distribution of the pores, pore shapes and morphologies, connectivity of the pores, and the nature of the electrolyte. In addition, the resistance to ion transport within the inner pores and a large diffusion distance can lead to a substantial IR drop, which becomes more significant at higher currents, adversely affecting the performance of the electrocatalysts. However, control over the pore size, its morphology, the generation of ordered mesopores and the combination of micropores and mesopores to give hierarchical micro-mesoporous carbon-based materials has the capacity to reduce the IR drops. Indeed, Dong et al. [72] observed an increase in the rate of the oxygen reduction reaction through the addition of micropores to disordered mesoporous activated carbon. It is now possible to design a variety of task-specific MCs, with tuneable pore sizes and morphologies, including hexagonal, cubic and cylindrical pores. Clearly, MC is an interesting material for electrochemical-based applications, its porosity, including the size and morphology of the mesopores can be controlled, conductivity can be enhanced through graphitisation, it is cost-effective, and has good mechanical and chemical stability, and it is an environmentally acceptable material. Its role in serving as an electrocatalyst or as an electrocatalyst support for the technologically important oxygen reduction reaction (ORR) is now reviewed following a brief introduction and account of the ORR.

3. Oxygen reduction and evaluation of activity

The oxygen reduction reaction is one of the most widely studied and important electrochemical reactions, with applications extending from fuel cells and metal-air batteries to electro-Fenton-based technologies [33,34,73–75]. In these applications, both the anodic and cathodic reactions are important, however it is typically the ORR half reaction that becomes the limiting and rate-determining reaction. The slow kinetics of the ORR affects significantly the performance of metal-air batteries and fuel cells and in recent years there has been tremendous interest in both the theoretical and experimental aspects of the ORR at different electrocatalysts [73,75–77].

The reduction of oxygen can proceed through a four electron or two

electron reduction reaction as illustrated in Eqs. (1) and (2) for the four electron transfer and Eqs. (3) and (4) for the two electron transfer reaction [73]. The four-electron reduction reaction is the thermodynamically favoured reaction with a standard reduction potential of 1.23 V vs. SHE, and is an essential half reaction in fuel cells, where oxygen is used as the fuel. On the other hand, the *in situ* electrochemical formation of H_2O_2 is achieved through the two electron reduction of oxygen, and this is a key reaction in electro-Fenton, which is an important advanced oxidation technology with applications in wastewater treatment [33, 34].

$$O_2 + 4H^+ + 4e^- \rightarrow 2H_2O(\text{acidic}) \qquad E^0 = 1.23\text{V vs.SHE} \tag{1}$$

$$O_2 + 2H_2O + 4e^- \rightarrow 4OH^-(\text{alkaline}) \qquad E^0 = 0.40\text{V vs.SHE} \tag{2}$$

$$O_2 + 2H^+ + 2e^- \rightarrow H_2O_2(\text{acidic}) \qquad E^0 = 0.70\text{V vs.SHE} \tag{3}$$

$$O_2 + H_2O + 2e^- \rightarrow OOH^- + OH^-(\text{alkaline}) \qquad E^0 = 0.06\text{V vs.SHE} \tag{4}$$

The reduction of oxygen at carbon-based electrodes is generally described by the associative mechanism, which is summarised by Eqs. (5) to (9) for the four electron reduction reaction to give water as the final product and Eq. (10) for the production of hydrogen peroxide. Here the oxygen molecule is adsorbed and this adsorption step depends on the availability of free surface active sites for O_2 adsorption. The adsorption of O_2 is in competition with the adsorption of OH^- ions from water and therefore active sites that favour the adsorption of O_2 are crucial in this first step. It has been suggested that the selectivity of the two competing ORR reactions, i.e., the four and two electron reduction reactions, is determined by the relative prevalence of Eqs. (7) and (10) [78]. In addition, hydrogen peroxide can decompose into water as illustrated in Eq. (11), making it difficult to electrochemically generate H_2O_2.

$$O_2 \rightarrow {}^*O_2 \tag{5}$$

$${}^*O_2 + H^+ + e^- \rightarrow {}^*OOH \tag{6}$$

$${}^*OOH + H^+ + e^- \rightarrow H_2O + {}^*O \tag{7}$$

$${}^*O + H^+ + e^- \rightarrow {}^*OH \tag{8}$$

$${}^*OH + H^+ + e^- \rightarrow H_2O \tag{9}$$

$${}^*OOH + H^+ + e^- \rightarrow H_2O_2 \tag{10}$$

$$2H_2O_2 \rightarrow 2H_2O + O_2 \tag{11}$$

In terms of kinetics, it has been suggested that the rate-determining step is the adsorption of the oxygen molecules, Eq. (5), for strongly binding metals/alloys. On the other hand, for weakly binding electrocatalysts, Eq. (6) becomes the rate-determining step [78]. Eq. (8)

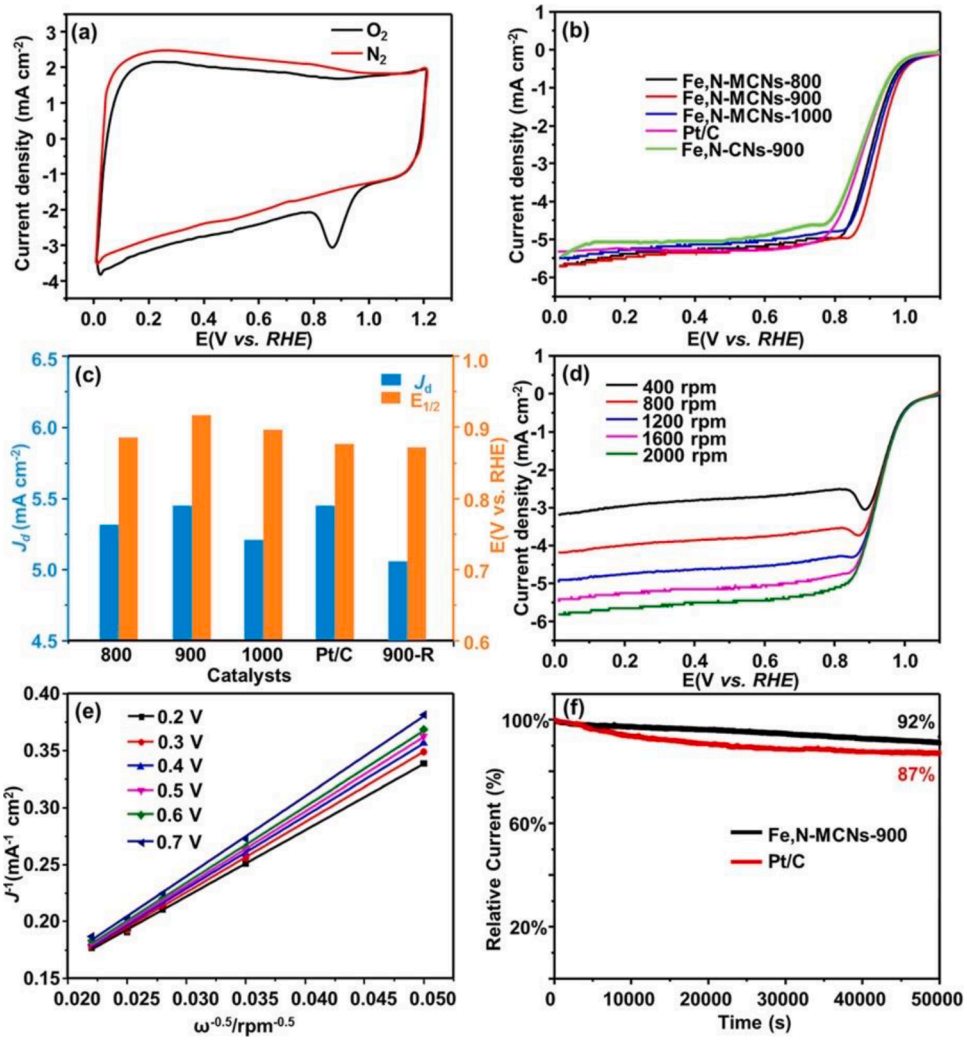

Fig. 2. **(a)** CV for Fe,N-MCNs in 0.1 M KOH solution saturated with Ar and O_2, **(b)** ORR polarisation curves for Fe,N-MCNs prepared at different temperatures and compared with commercial Pt/C, **(c)** J_d at 0.50 V and $E_{1/2}$ of the catalysts formed at different temperatures, **(d)** polarisation curves of Fe,N-MCNs at various rotating rates in 0.1 M KOH solution, **(e)** K–L fitted plots at various potentials for Fe,N-MCNs, **(f)** Durability studies at 0.3 V vs RHE comparing Fe,N-MCNs and commercial Pt/C, reprinted with permission from the American Chemical Society and taken from Du et al. [79].

The performance of electrocatalysts in the ORR is normally assessed using electrochemical techniques, such as cyclic voltammetry, linear sweep voltammetry and rotating disc electrode (RDE) experiments [77,78,81]. As illustrated in Fig. 2(a), the potential at which the reduction of dissolved oxygen occurs can be readily obtained using cyclic voltammetry. In the RDE experiment, a linear sweep voltammogram is recorded at slow scan rates, typically between 1 and 10 mV s^{-1} and at about 1600 rpm. A sigmoidal wave typical of the steady-state mass transport is obtained as shown in Fig. 2(b). From these RDE experiments, the E_{Onset} value can be determined. It is frequently (but not always) defined as the potential at which the current density for the ORR reaches the threshold of 0.1 mA cm^{-2}. Another useful parameter is the $E_{½}$ potential, which corresponds to the half-wave potential. The limiting current, J_L, is given by the Levich equation, Eq. (12), where D is the diffusion coefficient,ν is the kinematic viscosity, ω is the angular velocity of rotation, and the other symbols n, F, A and C, correspond to the number of electrons transferred, Faraday's constant, the geometric surface area of the electrode and concentration of electroactive species [77]. The Koutecký-Levich equation, Eq. (13), is also frequently applied, where J_K represents the kinetic current and J_L is the diffusion-limited current. A typical plot is shown in Fig. 2(e). Using this relationship, the rate constant k_e and the number of electrons transferred, n, can be obtained. This in turn can be used to determine the level of selectivity for the four and two electron transfer reactions. Electrocatalysts with higher ORR activity tend to give higher E_{Onset} values and higher $E_{½}$ values, while the limiting currents depend mainly on the n value [77,78].

$$J_L = 0.62nFAD^{2/3}\omega^{1/2}\nu^{-1/6}C \tag{12}$$

$$\frac{1}{J} = \frac{1}{J_K} + \frac{1}{J_L} = \frac{1}{nFAk_eC} + \frac{1}{J_L} \tag{13}$$

Tafel slopes obtained by fitting experimental data to the Tafel equation, Eq. (14), where b is the Tafel slope ($b = 2.303RT/\alpha F$) are also frequently employed. The Tafel slope is related to the overpotential required to increase the current density by one order of magnitude. It can also be employed to give insights into the reaction mechanism and the rate-determining steps [80].

$$\eta = a + b\log J \tag{14}$$

Currently, the best performing electrocatalysts are based on supported platinum nanoparticles with Pt/C being the most successful and commercially available [75]. Platinum-based electrocatalysts are not only expensive, but also the platinum nanoparticles are prone to leaching from the carbon support, which leads to secondary pollution while CO poisoning during the electrochemical reaction can reduce the overall performance of the cell. Furthermore, the availability of platinum is becoming an issue, as the Earths reserves are becoming depleted due to the excessive use of platinum in modern industries. Therefore, there is increasing interest in the development of more sustainable ORR electrocatalysts from Earth abundant elements that are cost-effective and readily scalable. It is no surprise that carbon-based materials, including MC and OMC are attracting considerable interest in the development of ORR electrocatalysts, as they are environmentally acceptable, inexpensive with very good stability and are readily available [81,82].

4. Metal-free heteroatom doped mesoporous carbon and the ORR

In general, the strategy to develop highly efficient carbon-based materials involves tuning of the pore size, the introduction of defects, such as intrinsic carbon defects, and defects arising from doping and graphitisation, aiming to enhance the surface area and to provide sufficient active sites for the electrochemical ORR [83,84]. During the last two decades, MCs and OMCs, with their fascinating properties of high surface areas, large pore volumes, and a tuneable nanostructure, have been shown to exhibit superior electrochemical ORR behaviour [85]. In testing the ORR activity of the electrocatalysts using the RDE setup, the MC-based electrocatalysts are normally dispersed in a solvent (e.g. water or alcohol) and a small amount of Nafion or other ionomer is added, which acts as a binder. Then they are deposited onto a substrate electrode, such as a glassy carbon surface, with catalyst loadings varying from approximately 25 μg cm^{-2} to 600 μg cm^{-2} [38,86–88].

It is well established that pristine carbon-based materials exhibit low electrocatalytic activity for the ORR [89], but the ORR activity is much higher when defects are introduced and this can be achieved by doping with heteroatoms. One well known dopant is nitrogen, and nitrogen doped OMCs and MCs have been investigated extensively [22,23,43,85,90–93]. Various nitrogen-based precursors can be employed as the nitrogen source in the fabrication of N doped MCs and OMCs. These include conducting polymers such as polyaniline, as it has a high N/C ratio [91,94], and polypyrrole [95], and graphitic carbon nitride, g-C_3N_4 as it releases large amounts of N-containing gases at high temperatures [27]. Other nitrogen sources include melamine [96], 2-pyridinecarboxaldehyde, pyrrole [19], folic acid [97], amino acids and poly amino acids as they are all rich in nitrogen [98]. There is also increasing interest in forming nitrogen-doped MC materials from biomass waste [99]. The nitrogen doping levels are typically between 3 and 9% [97,98,100] although higher levels have been achieved using a microwave assisted synthetic approach with a nickel foam substrate [96].

As the nitrogen atom is larger and has a higher electronegativity than carbon atoms, its incorporation into a carbon matrix gives rise to the polarisation of the matrix and the creation of defects. This leads to the generation of adsorption sites for the oxygen molecule, Eq. (5). It is also well known that the nature of the N functionalities can influence the rate of the ORR. On doping carbon with nitrogen, various N-containing centres can be generated, including pyridinic-N, pyrrolic-N and graphitic-N (quaternary N). There is a general consensus that it is the graphitic-N and also possibly the pyridinic-N that provide the active sites in N-doped carbon for the ORR [101]. However, these active sites need to be fully accessible to the reactants to ensure their utilisation. In addition to the nature of the N species, and pore accessibility, the ORR activity is also very dependent on the degree of graphitisation, which dictates the conductivity and stability of the doped carbon and also on the surface area, morphology of the porous structures and pore size distribution [102,103]. For example, Ferrero et al. [93] attributed the high performance of their nitrogen-doped MC microspheres to the relatively high nitrogen content of 8 wt%, an accessible mesoporosity that provides efficient mass transport both to and from the catalytic sites, a pore volume of 1.43 cm^3 g^{-1} and a large specific surface area of 1160 m^2 g^{-1}. Indeed, these materials were shown to outperform the commercial Pt/C electrocatalysts, with higher ORR activity, more robust characteristics and were unaffected by methanol crossover.

Other interesting dopants are P [90,95,104–109], S [32,110–117] and B [118–122] and these have been employed together with N-doping to enhance the ORR. In particular, co-doping with N and P or N and S gives higher ORR activity compared to N-doped carbon. Furthermore, it has been shown that multi-heteroatom doping, with N, P, and S, combined with an hierarchically porous carbon network outperformed the commercial Pt/C electrocatalyst in alkaline electrolytes [112]. The synthetic process of this ternary S, P, and N doped hierarchical carbon is summarised in Fig. 3. Interestingly, it has been shown that higher ORR activity can be achieved by first doping with P and then with N. This approach gave higher levels of graphitic-N, with some of the first doped P sites serving as locations for the N dopants [123]. Likewise, the co-doping with N and S is interesting, as the sulfur atom has a radius higher than either N or C. This, in turn, induces structural defects within the carbon framework to give more active sites for oxygen adsorption. Likewise, the presence of B dopants can alter the band structure of the carbon framework and facilitate the adsorption of oxygen [122].

Most of the reported ORR studies have been carried out in KOH and this is connected mainly with the fact that N-doped MC has higher ORR

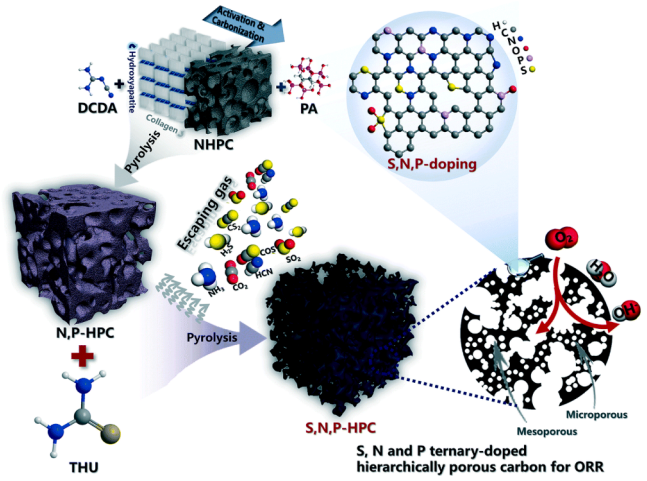

Fig. 3. Synthesis of S, N, P doped hierarchical porous carbon through the pyrolysis of thiourea (THU), with N- and P-doped porous carbon derived from cattle bone, reprinted with permission from RSC and taken from Zan et al. [112].

activities in alkaline compared to acidic media [91]. This is reflected in Table 1 where the performance of some MC materials with different heteroatom dopants is summarised. It is difficult to compare these directly as they have different pore structures, pore volumes, pore distributions and surface areas and have been formed using various approaches. Nevertheless, it is evident that some of best ORR activity is seen with N doped MC that has additional large pores [103,124] highlighting not only the influence of defects but also the important role of diffusion within the porous structures. In addition to the defects introduced by doping with heteroatoms, intrinsic carbon defects, such as edge defects and sp^3-type carbon, can also promote the ORR [125,126].

Table 1
Summary of some hetero-atom doped MC and their ORR activity in 0.1 M KOH.

Doping/Synthetic Process	Electrochemical Parameters	Refs.
N-doped/hydrothermal self-assembly	E_{onset} = −0.08 V vs. SCE Tafel slope = 73 mV/dec	[100]
N-doped/ direct pyrolysing (biomass source of carbon)	$E_{½}$= 0.75 V vs. RHE	[127]
N-doped/ solvent-free self-assembly	E_{onset} = 1.003 V vs. RHE $E_{½}$= 0.858 V vs. RHE Tafel slope = 70 mV dec^{-1}	[27]
N doped spheres/ micelles/high-molecular-weight block polymer	E_{onset} = −0.11 V vs. Ag/AgCl	[103]
N-doped hierarchical micro-MC/ templating	$E_{½}$= −0.243 V vs. SCE	[124]
N-doped/ SBA-15 template	E_{onset} = 0.9 V vs. RHE	[92]
N-doped OMC hollow spheres	E_{onset} = 0.88 V vs. RHE $E_{½}$ = 0.82 V vs. RHE	[19]
N-doped/ silica microspheres template.	E_{onset} = 0.927 V vs. RHE	[93]
N-Doped Hollow MC nanospheres	E_{onset} = 0.84 V vs. RHE Tafel slope = 65 mV dec^{-1}	[128]
N and S co-doping/soft template method	$E_{½}$ = 0.81 V vs. RHE	[129]
N and O co-doped/ SBA-15 mesoporous silica template	E_{onset} = 0.94 V vs. RHE	[91]
N and S co-doped/ hydrothermal	E_{onset} = 0.79 V vs. RHE Tafel slope, 72.0 mV dec^{-1}	[130]
N, P and S tri-doped MC/template	E_{onset} = 0.923 V vs. RHE $E_{½}$ = 0.821 V vs. RHE	[131]
B-doped/ SBA-15 hard template	E_{onset} = −0.16 V vs. Ag/AgCl	[122]
B and N co-doped /hydrothermal	E_{onset} = 0.975 V vs. RHE Tafel slope = 89.5 mV dec^{-1}	[132]

5. Modification of mesoporous carbon with transition metals

The presence of transition metals as both single atoms and nanostructures can further improve the ORR performance of the MC electrocatalysts. The influence of transition metal single atom electrocatalysts is summarised in Section 5.1, while incorporated transition metal nanostructures are described in Section 5.2. However, it should be noted that in many of these studies both centres co-exist, with both the atomic metal sites and nanoparticles contributing to the ORR.

5.1. *Single atomic transition metal modified mesoporous carbon and ORR*

Among the N-, P-, S- and B- heteroatom doped MC materials, non-precious single atom transition metal-containing N-doped MC comprise some of the more promising ORR electrocatalysts with performances comparable, or even superior, to the commercial Pt/C electrocatalysts in alkaline solutions. Transition metals such as Fe [31,79,88,133–136], Co [137–140], Mn [141,142], Ni [140] and various bimetallic combinations [133] are widely employed with N-doped MC/OMC, while Fe has also been employed with N, S co-doped MC [143]. There are fewer mentions of Ni, as it has been associated with a poisoning effect on the ORR activity [144]. In Fig. 4 the TEM micrograph of a Co-N-MC electrocatalyst is shown, together with the elemental mapping, indicating uniformly doped MC, while the linear sweep voltammograms illustrate how Co-N-MC, Cu-N-MC and Ni-N-MC, compare with the commercial Pt/C electrocatalysts [140]. In Table 2, the performance of some of these single atom-based MC electrocatalysts is summarised. In general, the E_{Onset} potentials are in the vicinity of 1.0 V vs. RHE, while many of the $E_{½}$ values are higher than 0.90 V vs. RHE. On comparing these values with the data presented in Table 1, it is evident that the single atom transition metal modified MC-based electrocatalysts are generally more efficient in facilitating the ORR.

It is believed that the transition metal (M) coordinates to the nitrogen moieties to give M-N_x active centres, that are covalently bonded to the carbon structure. This facilitates the adsorption of oxygen and its reaction intermediates with the metal centre through electron-donating or -withdrawing with the π-electron system of the carbon support. In the case of the combination of Fe with S and N doped MC, the impressive ORR activity was attributed to the dual N, S doping, Fe-N_x and possibly FeS [143]. Likewise, it was deduced that Co-N_x sites can effectively boost the ORR in Co and N modified MC [145]. Nevertheless, these sites must be accompanied by high surface areas and pore volumes to enable the adsorption of the oxygen molecule at the active sites, coupled with efficient transport of electrolyte, reactants and products to and from the active sites, and high concentrations of pyridinic-N and graphitic-N species [145]. Therefore, it is not surprising that the ORR activity of transition metal and N doped MC or OMC depends strongly on the synthetic methodologies employed to integrate the nitrogen, carbon and the transition metal. Parameters such as the nature of the nitrogen and carbon precursors, transition metals, heating and post treatments are all important in dictating the properties of the final product [143].

In a recent study, Lilloja and co-workers [133] doped a commercial mesoporous engineered catalyst support with nitrogen and bimetallic CoFe, FeMn, and CoMn. Phenanthroline was employed as the nitrogen source, as it is also well known to form complexes with transition metal salts. Using XPS, the authors found that the nitrogen was present as graphitic-N, pyridinic-N, and pyrrolic-N but also a considerable amount of metal-coordinated nitrogen species were identified. The materials containing iron, exhibited impressive ORR activity similar to that of commercial Pt/C with E_{onset} and $E_{1/2}$ values of approximately 1.0 V and 0.9 V vs. RHE, respectively. Likewise, Wang et al. [31] observed very impressive ORR activity in 0.1 M KOH using Fe with N-doped MC. A $E_{1/2}$ of 0.926 V vs. RHE and an impressive current density of 92.5 mA cm^{-2} at 0.85 V was reported. Furthermore, very good long-term stability was achieved over a 90 h period with over 90% of the activity retained.

While the metal-N_x structures provide active adsorption sites with

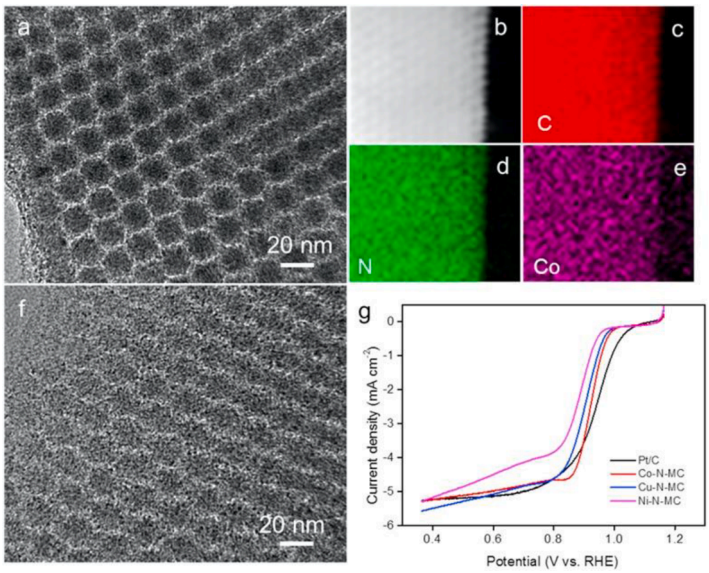

Fig. 4. **(a)** TEM image of the Co-N-MC, **(b)** HAADF-STEM image of the Co-N-MC, **(c)** carbon element mapping, **(d)** N element mapping, and **(e)** Co element mapping of as-prepared Co-N-MC, **(f)** TEM image of the as-prepared Cu-N-MC, **(g)** LSV curves for Co-N-MC, Ni-N-MC, Cu-N-MC, and Pt/C in O_2–saturated 0.1 M KOH at 10 mV s^{-1} and 1600 rpm, reprinted with permission from Elsevier and taken from Tang et al. [140].

Table 2
Summary of some MCs with single atom transition metals and their ORR activity in KOH.

Electrocatalysts	C precursors	Electrochemical Parameters	Refs.
Fe-N_x graphitic carbon	2,2-bipyridine	E_{Onset} = 0.97 V vs. RHE	[67]
Fe - N doped MC	polyvinyl-pyrrolidone	E_{Onset} = 0.99 V vs. RHE $E_{½}$ = 0.92 V vs. RHE	[79]
Co,Fe - N doped MC	1,10-phenanthroline	E_{Onset} = 1.0 V vs. RHE $E_{½}$ = 0.9 V vs. RHE	[133]
Fe - N doped MC	nicarbazin	E_{Onset} = 0.99 V vs. RHE	[134]
Fe-doped MC	glucose	E_{Onset} = 1.02 V vs. RHE $E_{½}$ = 0.84 V vs. RHE Tafel slope = 93 mV dec^{-1}	[136]
Co - N doped MC	polyvinyl-pyrrolidone	$E_{½}$ = 0.82 V vs. RHE Tafel slope = 51.8 mV dec^{-1}	[137]
Co - N,P doped MC, (single Co-N_2P_2 sites)	hexachloro-cyclotriphosphazene and tannic acid	$E_{½}$ = 0.878 V vs. RHE	[139]
Mn - N doped MC	phenanthroline	E_{Onset} = 0.96 V vs. RHE $E_{½}$ = 0.86 V vs. RHE	[141]
FeS - N, S doped MC	tetramethoxysilane and formic acid (sol-gel synthesis)	E_{Onset} = 1.00 V vs. RHE $E_{½}$ = 0.87 V vs. RHE Tafel slope = 74 mV dec^{-1}	[143]
Co - N doped MC	2,4,6-tri(2-pyridyl)–1,3,5-triazine	E_{Onset} = 1.0 V vs. RHE $E_{½}$ = 0.83 V vs. RHE	[145]

fast charge transfer, facilitating the ORR, they can be prone to corrosion and dissolution, especially in acidic environments. Indeed on testing the durability of Fe/N modified MC in H_2SO_4, Kwak et al. [88] observed a loss in both the N and Fe and a decreased portion of Fe-N_x which serves as the main active site. Therefore, most of these studies are carried out in alkaline KOH solutions.

Interestingly, there remains some debate concerning the intrinsic nature of the active site in N-doped carbon materials and this may also be very relevant for MC and OMC-based materials. In many of the synthetic methods, transition metals such as Fe-based salts are employed as cross-linking agents [59], and it has been argued by several authors that these transition metals may have a role to play in the ORR. It has been proposed that the transition metal promotes the formation of the catalytic sites during the pyrolysis reactions but is not actively involved in the ORR [146,147]. On the other hand, other groups argue that the transition metal coordinates with nitrogen and directly participates in the active sites for the ORR [148,149]. In a more recent study, Wan et al. [92] found no evidence to show that the iron-based salts used during the pyrolysis phase, played a role in the electrocatalysis of the ORR at MC or OMC.

5.2. *Mesoporous carbon as a support for nanostructured electrocatalysts*

Mesoporous carbon has also been shown to provide an effective support for transition metal nanoparticles, transition metal alloy nanostructures and indeed other nanosized electrocatalysts [150–153]. It provides a conducting support with an efficient electron transport pathway, while facilitating coupling between the transition metal electrocatalyst and the carbon to enhance the catalytic performance. It is well known that nanoparticles are prone to aggregation or agglomeration. However by immobilising them in a conductive support, such as MC, these self-aggregation reactions can be minimised to enhance the stability and electrocatalytic properties of the nanostructures. Again, heteroatom doping, to give N-doped MC supports, is interesting as the heteroatoms can influence the distribution of electron density and provide active adsorption sites. Furthermore, bonds between the heteroatoms and metal atoms can be formed which in turn can create polarity and charge distribution to enhance the electrocatalytic activity and the ORR performance.

Nevertheless, blocking of the pore space by the nanoparticles can reduce the diffusional processes that are necessary to achieve efficient transport of the reactants and products during the ORR. In particular, efficient transport between the pores and the bulk solution is required to ensure that the active sites are electrochemically accessible. In addition, the nitrogen doped carbon with metal nanoparticles are typically synthesised by thermal treatments of the transition metal, nitrogen, and

carbon precursors. The high temperatures make it difficult to control the distribution and aggregation of the metal nanoparticles. Different strategies have been employed to protect the transition metal nanoparticles and one method involves their protection by a thin carbon layer [154, 155], as shown in Fig. 5(a). This is particularly important when the nanoparticles are exposed to high temperatures and the aggressive etching conditions that are employed to remove the templates. Under these aggressive conditions, the transition metal nanoparticles can undergo dissolution and corrosion. Furthermore, the protection of the nanoparticles by a carbon layer can increase the long-term durability of the electrocatalytic nanoparticles and this is especially relevant in acidic media.

Another approach involves a low temperature synthesis to prepare the dispersed metal catalysts in the solution phase prior to the higher temperature processing [158]. By controlling the temperature, more control over the nucleation of the nanoparticles can be achieved while aggregation can be effectively suppressed.

Several nanoparticles and nanostructures have been successfully immobilised within MC to give impressive ORR activity and these include a number of iron-based nanostructures, including iron nanoparticles [159], Fe_3O_4 [160,161], Fe_2O_3 [162], Fe/Fe_2O_3 [163], FeCo [164], $CoFe_2O_4$ [165,166], $Fe_{1-x}S$ [167], Fe_3C [168–171], FeS [172], and Fe_2P [173,174] nanostructures. Similarly, a number of cobalt-based nanostructures have been employed, such as Co nanoparticles [175–180], single-atom-like Co with Co nanoparticles [181], CoO [182–184], Co/CoO [185], Co_3O_4 [186,187], CoP [153,188], CoCu

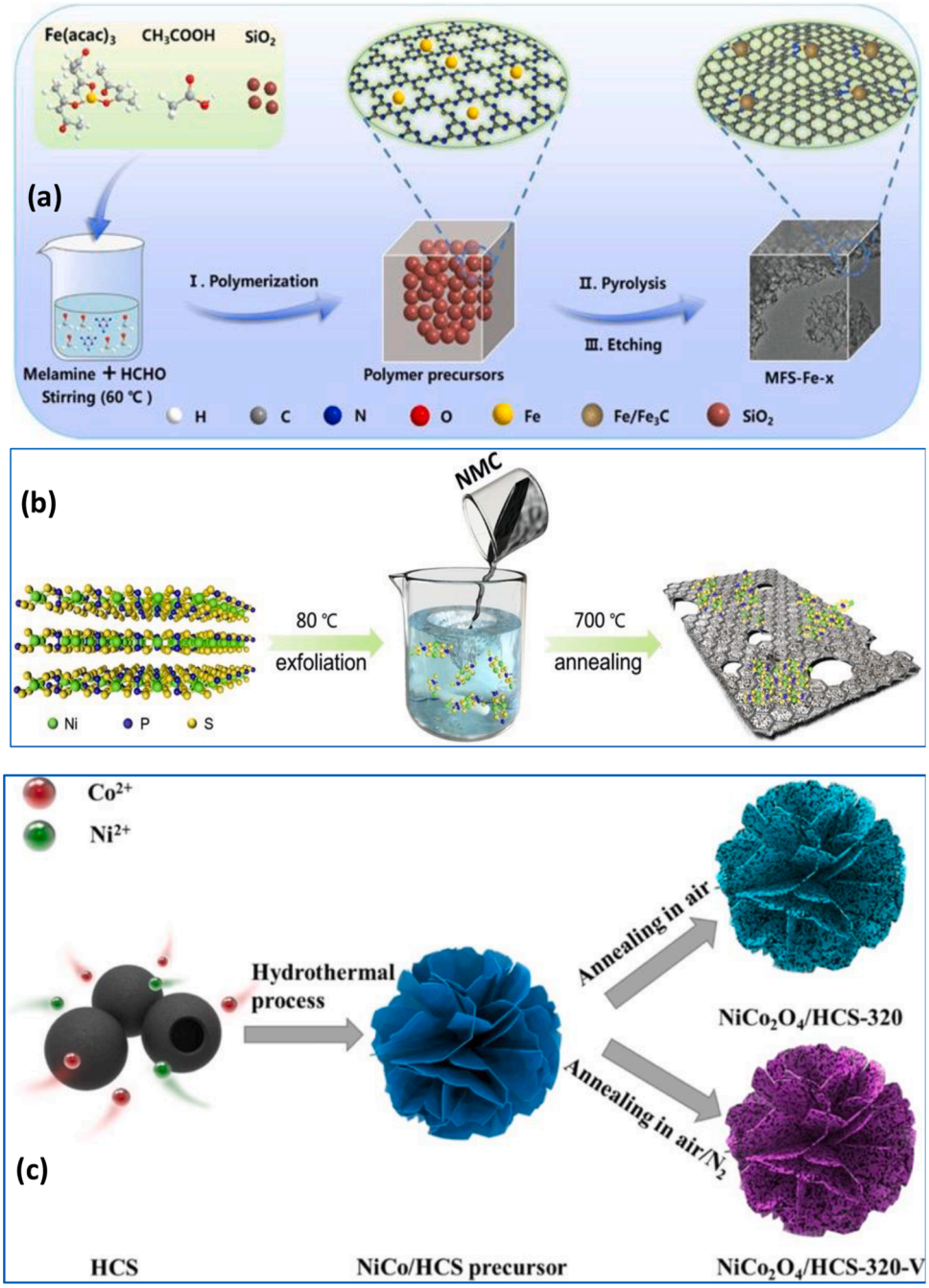

Fig. 5. Schematic of **(a)** the protection of metals by carbon layers and immobilised in MC, reprinted with permission from Elsevier and taken from Zhang et al. [154], **(b)** incorporation of trichalcogenides within MC, reprinted with permission from Elsevier and taken from Huang et al. [156], and **(c)** the preparation of $NiCo_2O_4$/HCS reprinted with permission from the American Chemical Society and taken from Yuan et al. [157].

[189], CoFe [190], CoS or Co_xS_y [191–195], CoSe [196,197], Co_9S_8 [198], CoNi [199], Co/CoS/Fe [200], Co-VN [201], $NiCo_2O_3$ [202], $CoFe_2O_4$ [165,203], $MnCo_2O_4$ [204], CoN/CoO [205], $Co(II)_{1-x}Co_{x/3}Mn(III)_{2x/3}S$ [206] and $Co_{½}Fe_{½}S$ [207] nanostructures. A similar approach has been employed with the nickel-based systems, with the nanostructures comprising amorphous nickel oxides [208], spinel-type oxides [209–211], sulfides [212], binary metal sulfides ($NiCo_2S_4$) [213], rock salt type NiO—CoO solid solutions [202], and metal phosphorus trichalcogenides ($NiPS_3$) [156].

A summary of the activity of some of these electrocatalysts is provided in Table 3. It is difficult to directly compare these materials as a variety of carbon precursors are employed together with different synthetic methodologies. Nevertheless, many of the E_{Onset} and $E_{½}$ values are >0.95 V and > 0.90 V vs. RHE, respectively. On comparing Tables 1–3, it is evident that doping of the MC with nitrogen and the presence of single atom transition metals or nanostructures is beneficial. Indeed, it is generally accepted that the M-N_x/C, where M is Fe, Co or Mn, provides the active sites for the ORR [171,204].

In addition to the oxides and sulfides, other transition metal species have been employed. Recently, trichalcogenides, which are held together by Van der Waals forces, but can be exfoliated into two dimensional sheets, as illustrated in Fig. 5(b), have been used successfully. Transition metals with a spinel structure (AB_2O_4, where A and B are transition metals), such as MFe_2O_4 or MCo_2O_4, are also emerging as promising electrocatalysts for the ORR [214]. The spinel oxides exhibit good electrical conductivities due to the different valence states of the metals, but this conductivity can be further improved by combining them with highly conducting supports. It is no surprise that they have been incorporated and immobilised into MC supports [165,166]. Interestingly, Yuan et al. [157] fabricated mesoporous $NiCo_2O_4$ assembled on hollow carbon spheres, as illustrated in Fig. 5(c), and then introduced oxygen vacancies into the electrocatalyst by annealing in an oxygen-deficient atmosphere. Good performance was achieved, with E_{onset} of 0.90 V vs. RHE, $E_{1/2}$ of 0.78 V vs. RHE and a diffusion-limited current density of 5.8 mA cm^{-2}. The hollow carbon support was essential, while the oxygen vacancies enhanced the performance of the ORR.

Table 3
Summary of some transition metal nanoparticles (NPs) anchored to MC and their ORR activity in KOH.

Electrocatalysts	C precursors	Electrochemical Parameters	Refs.
Fe_2O_3—N-MC	dopamine	E_{Onset} = −0.050 V vs. Ag/AgCl $E_{½}$ = −0.15 V vs. Ag/AgCl	[162]
Fe_3O_4—N-MC	p-phenylenediamine	E_{Onset} = 0.93 V vs. RHE $E_{½}$ = 0.83 V vs. RHE Tafel slope = 70 mV dec^{-1}	[160]
$CoFe_2O_4$—N-MC	albumin	E_{Onset} = 0.98 V vs. RHE $E_{½}$ = 0.85 V vs. RHE	[165]
$CoFe_2O_4$_MC	furfuryl alcohol and oxalic acid	E_{Onset} = −0.23 V vs. Ag/AgCl Tafel slope = 99 mV dec^{-1}	[166]
$Fe_{1-x}S$-N,S-MC	melamine and poly (vinyl alcohol)	E_{Onset} = 0.989 V vs. RHE $E_{½}$ = 0.84 V vs. RHE Tafel slope = 79 mV dec^{-1}	[167]
Fe_3C—N-MC	g-C_3N_4 and polyaniline	E_{Onset} = 1.22 V vs. RHE $E_{½}$ = 0.888 V vs. RHE	[168]
Fe_3C-Fe-N-doped MC	glucose and urea	E_{Onset} = 0.99 V vs. RHE Tafel slope = 55 mV dec^{-1}	[170]
Co-Co-N_x C	polyacrylonitrile, pyrrole	E_{Onset} = 1.05 V vs. RHE $E_{½}$ = 0.799 V vs. RHE Tafel slope = 124 mV dec^{-1}	[177]
CoO—Co-N MC	dicyandiamide	E_{Onset} = 0.80 V vs. RHE $E_{½}$ = 0.78 V vs. RHE Tafel slope = 68 mV dec^{-1}	[182]
Co_3O_4—N-O MC	aniline/polyaniline	$E_{½}$ = 0.82 V vs. RHE Tafel slope = 78 mV dec^{-1}	[186]
CoS_x-N-O MC	glucose	$E_{½}$ = 0.835 V vs. RHE Tafel slope = 97mV dec^{-1}	[191]
$Co_{0.88}Se$-N-MC	peptone	E_{Onset} = 0.981 V vs. RHE $E_{½}$ = 0.826 V vs. RHE	[197]
$MnCo_2O_4$—N,S-MC	carboxymethyl cellulose	E_{Onset} = −0.079 V vs. Ag/AgCl $E_{½}$ =−0.160 V vs. Ag/AgCl	[204]

6. Four and two electron transfer at the mesoporous carbon-based electrocatalysts

Despite the promising electrocatalytic activity of MC and OMC-based electrocatalysts, it remains challenging to predict or indeed design an electrocatalyst with high selectivity for the four or two electron transfer ORR. Most electrocatalysts promote both reactions with the production of water and hydrogen peroxide. Furthermore, electrocatalysts that are efficient in the formation of H_2O_2, are often active for the further reduction of H_2O_2 to H_2O. It is generally accepted that the *OOH adsorbed intermediate plays a central role in the pathway of the ORR, with its binding energy depending on the composition of the electrocatalyst. The selectivity towards H_2O_2 depends on two competing reactions involving the *OOH species, Eqs. (7) and (10). These two pathways differ depending on how the *OOH is reduced, with the breakage of the *O*−OH bond leading to the production of H_2O, while the breakage/de-adsorption of the *−OOH, keeping the O−O bond intact, gives H_2O_2. Nevertheless, there are materials which have excellent selectivity for H_2O_2, but computational studies indicate that the breakage of O−OH is more facile than *−O [215]. This highlights the complexity, involving both thermodynamic and kinetic aspects, of this seemingly simple reduction reaction.

In Table 4 the results from a number of recent studies are summarised, with the selectivity or experimentally determined n values, where a value close to 2.0 indicates excellent selectivity for the hydrogen peroxide reaction, while a value in the vicinity of 4.0 signifies the production of water. It appears from this table that in the absence of transition metals and their active sites, N-doped MC favours the production of H_2O_2, but this can be altered with the addition of iron. Indeed, Roldán et al. [216] showed that the addition of even minor amounts of iron to N-doped MC favoured the four-electron reduction reaction giving rise to a mixed four- and two-electron transfer mechanism. As illustrated in Table 4, the incorporation of Fe–N_x and Fe_3C into MC is very effective in producing H_2O as the main product with very good selectivity for the four electron-transfer process. On the other hand, it appears that the addition of oxygenated species, for example to give Co-O-C, favours high selectivity for the two electron transfer reaction, as displayed in Fig. 6 [178,217]. Indeed, it has been shown using computational studies, that a lower energy barrier exists for the adsorption of *OOH on COOH-terminated carbon. This in turn promotes the generation of H_2O_2 with very good selectivity [7].

Nevertheless, there are some conflicting reports on the selectivity of these transition metal modified N doped carbon materials. For example, there are variations on the role of cobalt, with some reports concluding that Co-N-C is capable of promoting the four-electron pathway [145,181,185], while others indicate that it favours the two electron-transfer reaction [218]. Likewise, MnO-containing mesoporous nitrogen-doped carbon has been shown to trigger the four electron transfer reaction [219], but it has also been shown to exhibit selectivity for the two electron ORR [142]. It has also been shown that NiO_x is efficient and selective towards the two-electron oxygen reduction reaction when

Table 4
Summary of recent electrocatalysts with selectivity for the two and four electron transfer reduction of oxygen.

Materials/ C precursors	Textural properties	Dopant	selectivity / n	Refs.
MC/ SiO_2 template/(1 methyl-1H-pyrrole-2-yl) methanol	pore size = 3–4 nm	N	90% H_2O_2	[23]
MC/ 1-Ethyl-3-methylimidazolium dicyanamide	specific surface area (SSA) = 1300 $m^2 g^{-1z}$ eta potential = 20 mV	N	95–98% $n = 2.1$	[221]
OMC/SBA-15 silica with aniline, dihydroxynaphthalene	SSA = 877 m^2g^{-1} pore size = 3.3 nm	N	$n = 2.4$	[86]
MC/ silica template with phenanthrene or 1,10 phenanthroline or phenothiazine	SSA = 823–972 $m^2 g^{-1}$ pore size = 3.6 nm	N, S	$n = 2.5$	[32]
MC/silica with 1,10-phenanthroline, phenothiazine, dibenzothiophene	SSA = 881 m^2g^{-1}	N, S	80% H_2O_2	[222]
MC/ silica with polyaniline, or polypyrrole	pore size = 33 nm	N, S	$n = 2.0$	[216]
MC/ SiO_2 template with resorcinol	pore size = 5.48 nm	C–O groups	90% H_2O_2	[87]
MC/soft template, resorcinol and Pluronic, H_2O_2	pore size = 4 nm	C-O groups	94% H_2O_2	[7]
MC/ cigarette filters	pore size = 13–16 nm	N, B	$n = 3.96$	[118]
MC/silica with dopamine and phytic acid	SSA = 676 $m^2 g^{-1}$	N, P	$n = 3.4$	[223]
MC/silica with dopamine	SSA = 1068 $m^2 g^{-1}$ pore size = 11.4 nm	N	$n = 3.8$	[224]
MC/ resol, triblock copolymer as soft template and SiO_2, iron-functionalised resin	pore size = 3 nm with micropores	N	$n = 3.8$	[225]
MC/ dopamine, graphene oxide	pore size = 42 nm SSA = 98.65 $m^2 g^{-1}$	Fe/N Fe_3C	$n = 3.6$	[226]
MC/ mesoporous silica, Furfuryl alcohol, oxalic acid	pore size = 3.84 1103 $m^2 g^{-1}$	$NiCo_2O_4$	$n = 3.9$	[166]
MC/ SBA 15, 1,10-phenanthroline	pore size = 9.2 nm SSA = 533 $cm^2 g^{-1}$	Fe–N_x	$n = 3.7$	[227]
MC/ phenanthroline, melamine	SSA = 705 $m^2 g^{-1}$ pore size = 2 nm	Fe_3C, N	$n = 4.0$	[228]
MC/ pyrrole, aniline	–	N, S, $Fe_{1/2}Co_{1/2}S$	$n = 3.81$	[229]
MC/ polyvinylpyrrolidone, citric acid, glycine	–	Fe-N, Fe_3N	$n = 3.71$	[230]

immobilised in MC [208]. This was attributed to end-on adsorption of the *OOH intermediate at the amorphous NiO_x-C, favouring the two electron ORR process. On the other hand, Mao et al. concluded that Ni doping into Co-N-MC promoted the four electron transfer reaction [220].

Some of these conflicting variations may be due to the nature of the M-N_x sites, with different levels of M-N_2 and M-N_4, altering the adsorption of *OOH. The presence of intrinsic carbon defects, which depend on the synthetic approaches used in the fabrication of the MCs, may also alter the nature of the ORR [125,126]. Furthermore, these transition metal modified and nitrogen doped carbon-based electrocatalysts have been shown to produce water from the indirect oxygen reduction reaction, which involves two parallel reactions, the so called 2 + 2 reduction process, with H_2O_2 as an intermediate, Eqs. (15) and (16). Therefore, residence time within the pores can influence selectivity, with an increase in the residence time favouring this indirect process to yield the four-electron transfer reaction. Therefore, selectivity towards H_2O_2 may also be dependent on the mass transport within the mesopores.

$$O_2 + 2H^+ + 2e^- \rightarrow H_2O_2 \qquad E^0 = 0.68 \tag{15}$$

$$H_2O_2 + 2H^+ + 2e^- \rightarrow 2H_2O \qquad E^0 = 1.77 \tag{16}$$

In a recent study, Lee et al. [231], investigated the effect of the structure of a nitrogen-doped porous carbon network, comprising both mesopores and macropores, on the catalytic activity of Fe–N–C electrocatalysts, and showed that the four electron transfer reaction was favoured, with an n value of 3.9. They found that the mesopores and macropores played different roles, with the mesopores contributing to the generation of electrochemically active sites, while the macropores facilitated accessibility to the active sites. Interestingly, they concluded that the nature of the porous structure with interconnected macro, micro- and mesopores was the important characteristic with the surface area and the nitrogen content exerting less influence on the ORR. Similarly, Mo et al. [232], used space confinement in N-doped porous carbon spheres to promote the four electron transfer reaction. The authors concluded that the space confinement within the pores induced the further conversion of peroxides to water, facilitating the four electron transfer ORR. These studies highlight the role of the mesoporous structure in dictating the selectivity of the reduction of oxygen.

In summary, there is clear evidence to suggest that the selectivity of the ORR depends not only on the heteroatom dopants and transition metal M-N_x sites (Table 4), but also on the mesoporosity, interconnectivity and nature of the porous networks [232]. In general, the four electron ORR is favoured in the presence of Fe–N_x sites, while space confinements can further convert peroxides into water. On the other hand, N-doped or oxygen-containing MCs appear to follow the two-electron transfer mechanism.

7. Conclusion and future perspectives

In recent years, tremendous progress has been made in the fabrication of mesoporous, ordered mesoporous and hierarchically porous carbon-based materials. It is now possible to tailor the porosity, surface area, morphology, and surface chemistry of these materials. In particular, the hierarchical nanoarchitectures with an interconnecting porous network of mesopores, micropores and macropores offer low resistance to mass transport, making them also ideal in electrochemical-based applications. Not alone are these materials finding applications in the ORR, but they are attracting considerable interest as biomedical materials, supercapacitors, batteries, adsorbents in carbon capture, and sensors.

Before the full potential of these interesting materials is unlocked, further advances in their synthesis and especially in the scale-up of cost-effective synthetic methods that are environmentally acceptable is required. In this context, one emerging and interesting approach is the use of biomass precursors, which are low-cost, renewable and readily available. However, this requires further research, including mechanistic studies into the pyrolysis step, polymerisation processes, and the inclusion of *in-situ* appropriate dopants. In terms of environmental considerations, the hard template methods require the use of aggressive chemicals, such as HF and high concentrations of NaOH at elevated temperatures and therefore the soft template methods are more environmentally acceptable. More insights into how the mesoporous structure can influence performance are also needed in order to provide a

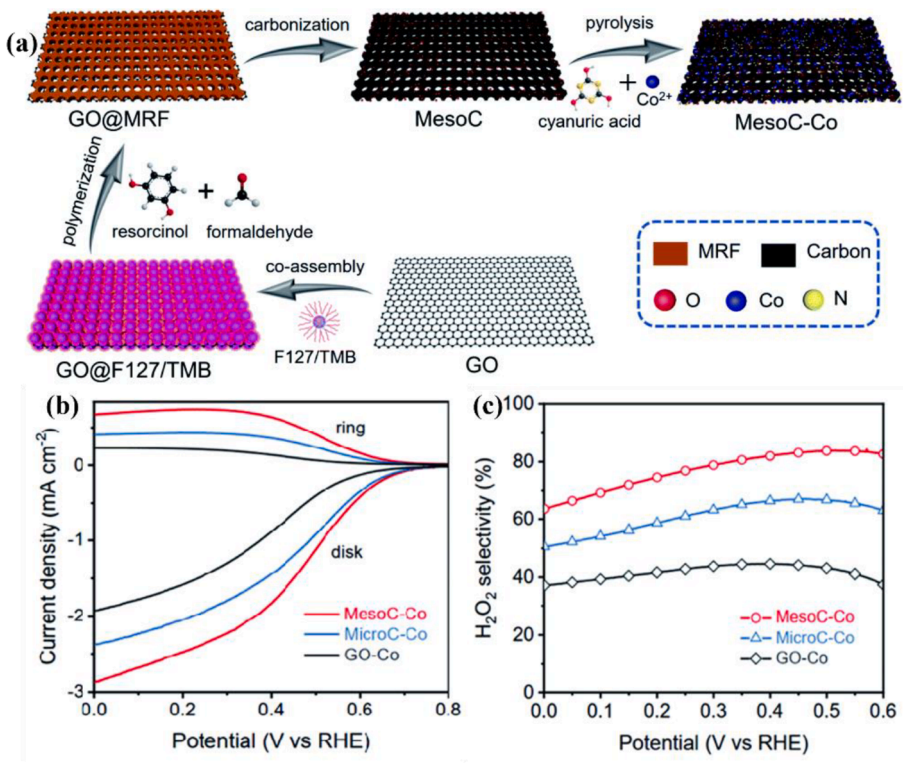

Fig. 6. **(a)** Synthesis procedure for mesoporous C—Co sample, **(b)** LSV curves of the three samples recorded at 1600 rpm in O_2-saturated 0.10 M $HClO_4$ and, **(c)** calculated H_2O_2 selectivity of the three samples at various potentials, reprinted with permission from RSC and taken from Jing et al. [217].

greater understanding of how to design tailor-made mesoporous materials for specific applications. In this context, a near atomic-level characterisation, involving *in-situ* real time spectroscopy and microscopy measurements coupled with computational studies would be beneficial.

Nevertheless, these materials, with appropriate dopants, such as N, P, S, and transition metals, including Fe, Co and Mn, have shown very good electrocatalytic activity in the ORR, with performances comparable or even higher than the commercial Pt/C electrocatalysts in alkaline solutions. It is also clear that the ORR activity depends on the nature and doping levels of the dopants, the surface area, the electronic conductivity and the mesoporosity. Therefore, there is clear potential to further optimise these electrocatalysts, by developing more control at the molecular level of the doping process and defect structure, while ensuring that there is no destruction of the mesoporous network or deterioration in the conductivity of the MC.

Although these doped MC-based electrocatalysts perform well, relatively little is known about the catalytically active sites and the specific role that they play in the mechanism of the ORR. Indeed, this can be seen when considering the selectivity of the mesoporous catalysts in the two- and four-electron transfer ORR, where in some cases similarly doped electrocatalysts have shown vastly different selectivity for the reduction of oxygen. It remains exceedingly challenging to control the defect structure and catalytically active sites and this, in turn, makes it more difficult to understand the precise role of the defects in the ORR. The MC and OCM electrocatalysts are typically prepared by pyrolysis-based methodologies making it difficult to control the nature of the defect structure and provide a direct link between the defects and the ORR activity. Clearly, the development of new approaches that can be used to control the nature of the defects is required. Only with these advances will a greater understanding of the role of the defects and active sites in the ORR be obtained. It is also evident that these MC-based materials can serve as effective supports for nanostructured electrocatalysts. However, more details on how these nanostructures are immobilised and held within the pores, or anchored to the surface is needed, while the precise roles of the nanostructures and the M-Nx catalytic sites in the ORR is currently lacking.

In terms of practical applications the stability of these materials is another important factor. Not only is the overall stability relevant, but so too is the stability of the defects and catalytic sites that promote the ORR. Currently, a clear understanding of how these sites evolve during the ORR is not available and this will require *in-situ* characterisation measurements.

In conclusion, MC-based materials with interesting mesoporous networks that can be readily doped and functionalised have clearly the potential to serve as electrocatalysts for the technologically important ORR. With further optimisation of these electrocatalysts, in terms of performance, cost and overall stability, it is likely that they will easily surpass the performance of the precious Pt-based carbon electrocatalysts in the very near future.

Declaration of Competing Interest

The authors declare that they have no known competing financial interests or personal relationships that could have appeared to influence the work reported in this paper.

Data availability

No data was used for the research described in the article.

Acknowledgments

This publication has emanated from research conducted with the financial support of Science Foundation Ireland under Grant number SFI/20/FFP-P/8793 and the Irish Research Council under grants number GOIPD/2022/694 and GOIPG/2022/1605.

Supplementary materials

Supplementary material associated with this article can be found, in the online version, at doi:10.1016/j.electacta.2022.141678.

References

[1] R. Taylor, D.R.M. Walton, The chemistry of fullerenes, Nature 363 (1993) 685–693, https://doi.org/10.1038/363685a0.

[2] L. Dai, D.W. Chang, J.B. Baek, W. Lu, Carbon nanomaterials for advanced energy conversion and storage, Small 8 (2012) 1130–1166, https://doi.org/10.1002/smll.201101594.

[3] C.N.R. Rao, B.C. Satishkumar, A. Govindaraj, M. Nath, Nanotubes, ChemPhysChem. 2 (2001) 78–105, https://doi.org/10.1002/1439-7641(20010216)2:2<78::AID-CPHC78>3.0.CO;2-7.

[4] Y. Chen, X. Bai, Y. Ji, T. Shen, Reduced graphene oxide-supported hollow Co_3O_4@N-doped porous carbon as peroxymonosulfate activator for sulfamethoxazole degradation, Chem. Eng. J. 430 (2022), 132951, https://doi.org/10.1016/j.cej.2021.132951.

[5] A. Ghaffarkhah, E. Hosseini, M. Kamkar, A.A. Sehat, S. Dordanihaghighi, A. Allahbakhsh, C. van der Kuur, M. Arjmand, Synthesis, applications, and prospects of graphene quantum dots: a comprehensive review, Small 18 (2022), 2102683, https://doi.org/10.1002/smll.202102683.

[6] B.J. Ostertag, M.T. Cryan, J.M. Serrano, G. Liu, A.E. Ross, Porous carbon nanofiber-modified carbon fiber microelectrodes for dopamine detection, ACS Appl. Nano Mater. 5 (2022) 2241–2249, https://doi.org/10.1021/acsanm.1c03933.

[7] C. Zhang, G. Liu, Q. Long, C. Wu, L. Wang, Tailoring surface carboxyl groups of mesoporous carbon boosts electrochemical H_2O_2 production, J. Colloid Interface Sci. 622 (2022) 849–859, https://doi.org/10.1016/j.jcis.2022.04.140.

[8] W. Tian, H. Zhang, X. Duan, H. Sun, G. Shao, S. Wang, Porous carbons: structure-oriented design and versatile applications, Adv. Funct. Mater. 30 (2020), 1909265, https://doi.org/10.1002/adfm.201909265.

[9] R. Bakry, R.M. Vallant, M. Najam-ul-Haq, M. Rainer, Z. Szabo, C.W. Huck, G. K. Bonn, Medicinal applications of fullerenes, Int. J. Nanomed. 2 (2007) 639–649. https://www.scopus.com/inward/record.uri?eid=2-s2.0-46149113117&partnerID=40&md5=94618c538165952dcfbc4547dc0ea1d2.

[10] L. Agüí, P. Yáñez-Sedeño, J.M. Pingarrón, Role of carbon nanotubes in electroanalytical chemistry. A review, Anal. Chim. Acta 622 (2008) 11–47, https://doi.org/10.1016/j.aca.2008.05.070.

[11] J. Zhang, Z. Xia, L. Dai, Carbon-based electrocatalysts for advanced energy conversion and storage, Sci. Adv. 1 (2015), e1500564, https://doi.org/10.1126/sciadv.1500564.

[12] R.N. Queiroz, P. Prediger, M.G.A. Vieira, Adsorption of polycyclic aromatic hydrocarbons from wastewater using graphene-based nanomaterials synthesized by conventional chemistry and green synthesis: a critical review, J. Hazard. Mater. 422 (2022), 126904, https://doi.org/10.1016/j.jhazmat.2021.126904.

[13] R. Ryoo, S.H. Joo, S. Jun, Synthesis of highly ordered carbon molecular sieves via template-mediated structural transformation, J. Phys. Chem. B 103 (1999) 7743–7746, https://doi.org/10.1021/jp991673a.

[14] J. Lee, S. Yoon, T. Hyeon, S.M. Oh, K.B. Kim, Synthesis of a new mesoporous carbon and its application to electrochemical double-layer capacitors, Chem. Commun. (1999) 2177–2178, https://doi.org/10.1039/a906872d.

[15] C. Vix-Guterl, E. Frackowiak, K. Jurewicz, M. Friebe, J. Parmentier, F. Béguin, Electrochemical energy storage in ordered porous carbon materials, Carbon 43 (2005) 1293–1302, https://doi.org/10.1016/j.carbon.2004.12.028. N. Y.

[16] W. Shen, W. Fan, Nitrogen-containing porous carbons: synthesis and application, J. Mater. Chem. A 1 (2013) 999–1013, https://doi.org/10.1039/c2ta00028h.

[17] M.J. Bleda-Martínez, J.A. Maciá-Agulló, D. Lozano-Castelló, E. Morallón, D. Cazorla-Amorós, A. Linares-Solano, Role of surface chemistry on electric double layer capacitance of carbon materials, Carbon 43 (2005) 2677–2684, https://doi.org/10.1016/j.carbon.2005.05.027. N. Y.

[18] R. Liu, D. Wu, X. Feng, K. Müllen, Nitrogen-doped ordered mesoporous graphitic arrays with high electrocatalytic activity for oxygen reduction, Angew. Chem. Int. Ed. 49 (2010) 2565–2569, https://doi.org/10.1002/anie.200907289.

[19] J.C. Carrillo-Rodríguez, A.M. Garay-Tapia, B. Escobar-Morales, J. Escorcia-García, M.T. Ochoa-Lara, F.J. Rodríguez-Varela, I.L. Alonso-Lemus, Insight into the performance and stability of N-doped ordered mesoporous carbon hollow spheres for the ORR: influence of the nitrogen species on their catalytic activity after ADT, Int. J. Hydrog. Energy 46 (2021) 26087–26100, https://doi.org/10.1016/j.ijhydene.2021.01.047.

[20] S. Gao, Y. Liu, Z. Xie, Y. Qiu, L. Zhuo, Y. Qin, J. Ren, S. Zhang, G. Hu, J. Luo, X. Liu, Metal-free bifunctional ordered mesoporous carbon for reversible Zn-CO_2 batteries, Small Methods 5 (2021), 2001039, https://doi.org/10.1002/smtd.202001039.

[21] A. Eftekhari, Z. Fan, Ordered mesoporous carbon and its applications for electrochemical energy storage and conversion, Mater. Chem. Front. 1 (2017) 1001–1027, https://doi.org/10.1039/c6qm00298f.

[22] X. Wang, J.S. Lee, Q. Zhu, J. Liu, Y. Wang, S. Dai, Ammonia-treated ordered mesoporous carbons as catalytic materials for oxygen reduction reaction, Chem. Mater. 22 (2010) 2178–2180, https://doi.org/10.1021/cm100139d.

[23] J. Park, Y. Nabae, T. Hayakawa, M.A. Kakimoto, Highly selective two-electron oxygen reduction catalyzed by mesoporous nitrogen-doped carbon, ACS Catal. 4 (2014) 3749–3754, https://doi.org/10.1021/cs5008206.

[24] T. Sun, N. Shan, L. Xu, J. Wang, J. Chen, A.A. Zakhidov, R.H. Baughman, General synthesis of 3D ordered macro-/mesoporous materials by templating mesoporous silica confined in opals, Chem. Mater. 30 (2018) 1617–1624, https://doi.org/10.1021/acs.chemmater.7b04829.

[25] C. Xue, B. Tu, D. Zhao, Facile fabrication of hierarchically porous carbonaceous monoliths with ordered mesostructure via an organic organic self-assembly, Nano Res. 2 (2009) 242–253, https://doi.org/10.1007/s12274-009-9022-y.

[26] Y.L. Xie, Q.N. Guo, Improved electrochemical performance of mesoporous carbon via N/S doping, J. Solid State Electrochem. 26 (2022) 1013–1020, https://doi.org/10.1007/s10008-022-05145-7.

[27] X. Liu, Y. Zhou, C.L. Wang, Y. Liu, D.J. Tao, Solvent-free self-assembly synthesis of N-doped ordered mesoporous carbons as effective and bifunctional materials for CO_2 capture and oxygen reduction reaction, Chem. Eng. J. 427 (2022), https://doi.org/10.1016/j.cej.2021.130878.

[28] N. Gavrilov, M. Momčilović, A.S. Dobrota, D.M. Stanković, B. Jokić, B. Babić, N. V. Skorodumova, S.V. Mentus, I.A. Pašti, A study of ordered mesoporous carbon doped with Co and Ni as a catalyst of oxygen reduction reaction in both alkaline and acidic media, Surf. Coat. Technol. 349 (2018) 511–521, https://doi.org/10.1016/j.surfcoat.2018.06.008.

[29] X. Liu, W. Li, S. Zou, Cobalt and nitrogen-codoped ordered mesoporous carbon as highly efficient bifunctional catalysts for oxygen reduction and hydrogen evolution reactions, J. Mater. Chem. A 6 (2018) 17067–17074, https://doi.org/10.1039/c8ta06864j.

[30] S.H. Joo, S.J. Choi, I. Oh, J. Kwak, Z. Liu, O. Terasaki, R. Ryoo, Ordered nanoporous arrays of carbon supporting high dispersions of platinum nanoparticles, Nature 412 (2001) 169–172, https://doi.org/10.1038/35084046.

[31] X. Wang, H. Zhu, C. Yang, J. Lu, L. Zheng, H.P. Liang, Mesoporous carbon promoting the efficiency and stability of single atomic electrocatalysts for oxygen reduction reaction, Carbon 191 (2022) 393–402, https://doi.org/10.1016/j.carbon.2022.01.057. N. Y.

[32] V. Perazzolo, C. Durante, R. Pilot, A. Paduano, J. Zheng, G.A. Rizzi, A. Martucci, G. Granozzi, A. Gennaro, Nitrogen and sulfur doped mesoporous carbon as metal-free electrocatalysts for the *in situ* production of hydrogen peroxide, Carbon 95 (2015) 949–963, https://doi.org/10.1016/j.carbon.2015.09.002. N. Y.

[33] T. Yu, C.B. Breslin, Review—2D graphene and graphene-like materials and their promising applications in the generation of hydrogen peroxide, J. Electrochem. Soc. 167 (2020), 126502, https://doi.org/10.1149/1945-7111/abad6f.

[34] T. Yu, C.B. Breslin, Graphene-modified composites and electrodes and their potential applications in the electro-Fenton process, Materials 13 (2020) 2254, https://doi.org/10.3390/ma13102254 (Basel).

[35] H. Xu, H. Li, L. Xie, D. Zhao, B. Kong, Interfacial assembly of functional mesoporous carbon-based materials into films for batteries and electrocatalysis, Adv. Mater. Interfaces 9 (2022), 2101998, https://doi.org/10.1002/admi.202101998.

[36] M.R. Benzigar, S.N. Talapaneni, S. Joseph, K. Ramadass, G. Singh, J. Scaranto, U. Ravon, K. Al-Bahily, A. Vinu, Recent advances in functionalized micro and mesoporous carbon materials: synthesis and applications, Chem. Soc. Rev. 47 (2018) 2680–2721, https://doi.org/10.1039/c7cs00787f.

[37] C. Liang, Z. Li, S. Dai, Mesoporous carbon materials: synthesis and modification, Angew. Chem. Int. Ed. 47 (2008) 3696–3717, https://doi.org/10.1002/anie.200702046.

[38] V. Duraisamy, S. Venkateshwaran, R. Thangamuthu, S.M. Senthil Kumar, Hard template derived N, S dual heteroatom doped ordered mesoporous carbon as an efficient electrocatalyst for oxygen reduction reaction, Int. J. Hydrog. Energy 47 (2022) 40327–40339, https://doi.org/10.1016/j.ijhydene.2022.03.250.

[39] A.B. Fuertes, Synthesis of ordered nanoporous carbons of tunable mesopore size by templating SBA-15 silica materials, Microporous Mesoporous Mater. 67 (2004) 273–281, https://doi.org/10.1016/j.micromeso.2003.11.012.

[40] M. Enterría, F. Suárez-García, A. Martínez-Alonso, J.M.D. Tascón, Hierarchical micro-mesoporous carbons by direct replication of bimodal aluminosilicate templates, Microporous Mesoporous Mater. 190 (2014) 156–164, https://doi.org/10.1016/j.micromeso.2014.02.008.

[41] J. Lee, S. Yoon, S.M. Oh, C.H. Shin, T. Hyeon, Development of a new mesoporous carbon using an HMS aluminosilicate template, Adv. Mater. 12 (2000) 359–362, https://doi.org/10.1002/(SICI)1521-4095(200003)12:5<359::AID-ADMA359>3.0.CO;2-1.

[42] R.A.L. Sobrinho, G.R.S. Andrade, L.P. Costa, M.J.B. de Souza, A.M.G.P. de Souza, I.F. Gimenez, Ordered micro-mesoporous carbon from palm oil cooking waste via nanocasting in HZSM-5/SBA-15 composite: preparation and adsorption studies, J. Hazard. Mater. 362 (2019) 53–61, https://doi.org/10.1016/j.jhazmat.2018.08.097.

[43] W. Niu, L. Li, X. Liu, N. Wang, J. Liu, W. Zhou, Z. Tang, S. Chen, Mesoporous N-doped carbons prepared with thermally removable nanoparticle templates: an efficient electrocatalyst for oxygen reduction reaction, J. Am. Chem. Soc. 137 (2015) 5555–5562, https://doi.org/10.1021/jacs.5b02027.

[44] U. Jeong, H. Kim, S. Ramesh, N.A. Dogan, S. Wongwilawan, S. Kang, J. Park, E. S. Cho, C.T. Yavuz, Rapid access to ordered mesoporous carbons for chemical hydrogen storage, Angew. Chem. Int. Ed. 60 (2021) 22478–22486, https://doi.org/10.1002/anie.202109215.

[45] X. Wang, S. Chen, C. Liu, Y. Yu, M. Xie, X. Guo, High-temperature deoxygenation-created highly porous graphitic carbon nanosheets for ultrahigh-rate supercapacitive energy storage, J. Energy Chem. 71 (2022) 521–527, https://doi.org/10.1016/j.jechem.2022.03.051.

[46] X. Sun, L. Lu, Q. Zhu, C. Wu, D. Yang, C. Chen, B. Han, MoP nanoparticles supported on indium-doped porous carbon: outstanding catalysts for highly

efficient CO_2 electroreduction, Angew. Chem. Int. Ed. 57 (2018) 2427–2431, https://doi.org/10.1002/anie.201712221.
[47] J. Schuster, R. Köhn, A. Keilbach, M. Döblinger, H. Amenitsch, T. Bein, Two-dimensional-hexagonal periodic mesoporous polymer resin thin films by soft templating, Chem. Mater. 21 (2009) 5754–5762, https://doi.org/10.1021/cm901163t.
[48] Y. Meng, D. Gu, F. Zhang, Y. Shi, L. Cheng, D. Feng, Z. Wu, Z. Chen, Y. Wan, A. Stein, D. Zhao, A family of highly ordered mesoporous polymer resin and carbon structures from organic-organic self-assembly, Chem. Mater. 18 (2006) 4447–4464, https://doi.org/10.1021/cm060921u.
[49] T. Chen, T. Wang, D.J. Wang, H.R. Xue, J.Q. Zhao, X.C. Ding, S.C. Wu, J.P. He, Synthesis of ordered large-pore mesoporous carbon for Cr(VI) adsorption, Mater. Res. Bull. 46 (2011) 1424–1430, https://doi.org/10.1016/j.materresbull.2011.05.009.
[50] P. Li, Y. Song, Q. Guo, J. Shi, L. Liu, Tuning the pore size and structure of mesoporous carbons synthesized using an evaporation-induced self-assembly method, Mater. Lett. 65 (2011) 2130–2132, https://doi.org/10.1016/j.matlet.2011.04.081.
[51] J. Wei, Y. Deng, J. Zhang, Z. Sun, B. Tu, D. Zhao, Large-pore ordered mesoporous carbons with tunable structures and pore sizes templated from poly(ethylene oxide)-b-poly(methyl methacrylate), Solid State Sci. 13 (2011) 784–792, https://doi.org/10.1016/j.solidstatesciences.2010.03.008.
[52] Y. Deng, Y. Cai, Z. Sun, D. Gu, J. Wei, W. Li, X. Guo, J. Yang, D. Zhao, Controlled synthesis and functionalization of ordered large-pore mesoporous carbons, Adv. Funct. Mater. 20 (2010) 3658–3665, https://doi.org/10.1002/adfm.201001202.
[53] L. Liu, F.Y. Wang, G.S. Shao, Z.Y. Yuan, A low-temperature autoclaving route to synthesize monolithic carbon materials with an ordered mesostructure, Carbon 48 (2010) 2089–2099, https://doi.org/10.1016/j.carbon.2010.02.022. N. Y.
[54] H. Javed, S. Pani, J. Antony, M. Sakthivel, J.F. Drillet, Synthesis of mesoporous carbon spheres: via a soft-template route for catalyst supports in PEMFC cathodes, Soft Matter 17 (2021) 7743–7754, https://doi.org/10.1039/d1sm00450f.
[55] J. Li, C. Shi, A. Bao, J. Jia, Development of boron-doped mesoporous carbon materials for use in CO_2 capture and electrochemical generation of H_2O_2, ACS Omega 6 (2021) 8438–8446, https://doi.org/10.1021/acsomega.1c00197.
[56] X. Wan, Y. Li, H. Xiao, Y. Pan, J. Liu, Hydrothermal synthesis of nitrogen-doped ordered mesoporous carbon: via lysine-assisted self-assembly for efficient CO_2 capture, RSC Adv. 10 (2020) 2932–2941, https://doi.org/10.1039/c9ra09983b.
[57] Y. Fang, D. Gu, Y. Zou, Z. Wu, F. Li, R. Che, Y. Deng, B. Tu, D. Zhao, A low-concentration hydrothermal synthesis of biocompatible ordered mesoporous carbon nanospheres with tunable and uniform size, Angew. Chem. Int. Ed. 49 (2010) 7987–7991, https://doi.org/10.1002/anie.201002849.
[58] X. Wang, X. Liu, R.L. Smith, Y. Liang, X. Qi, Direct one-pot synthesis of ordered mesoporous carbons from lignin with metal coordinated self-assembly, Green Chem. 23 (2021) 8632–8642, https://doi.org/10.1039/d1gc03030b.
[59] X. Liu, Y. Wang, R.L. Smith, L. Liu, X. Qi, Synthesis of self-renewing Fe(0)-dispersed ordered mesoporous carbon for electrocatalytic reduction of nitrates to nitrogen, Sci. Total Environ. 836 (2022), 155640, https://doi.org/10.1016/j.scitotenv.2022.155640.
[60] A.B. Fuertes, S. Alvarez, Graphitic mesoporous carbons synthesised through mesostructured silica templates, Carbon 42 (2004) 3049–3055, https://doi.org/10.1016/j.carbon.2004.06.020. N. Y.
[61] P.V. Shanahan, L. Xu, C. Liang, M. Waje, S. Dai, Y.S. Yan, Graphitic mesoporous carbon as a durable fuel cell catalyst support, J. Power Sources 185 (2008) 423–427, https://doi.org/10.1016/j.jpowsour.2008.06.041.
[62] T.W. Kim, I.S. Park, R. Ryoo, A synthetic route to ordered mesoporous carbon materials with graphitic pore walls, Angew. Chem. Int. Ed. 42 (2003) 4375–4379, https://doi.org/10.1002/anie.200352224.
[63] S.H. Joo, C. Pak, D.J. You, S..A. Lee, H.I. Lee, J.M. Kim, H. Chang, D. Seung, Ordered mesoporous carbons (OMC) as supports of electrocatalysts for direct methanol fuel cells (DMFC): effect of carbon precursors of OMC on DMFC performances, Electrochim. Acta 52 (2006) 1618–1626, https://doi.org/10.1016/j.electacta.2006.03.092.
[64] C.H. Kim, D.K. Lee, T.J. Pinnavaia, Graphitic mesostructured carbon prepared from aromatic precursors, Langmuir 20 (2004) 5157–5159, https://doi.org/10.1021/la049602c.
[65] D.W. Wang, G. Zhou, F. Li, K.H. Wu, G.Q. Lu, H.M. Cheng, I.R. Gentle, A microporous-mesoporous carbon with graphitic structure for a high-rate stable sulfur cathode in carbonate solvent-based Li-S batteries, Phys. Chem. Chem. Phys. 14 (2012) 8703–8710, https://doi.org/10.1039/c2cp40808b.
[66] M. Liu, L. Gan, W. Xiong, F. Zhao, X. Fan, D. Zhu, Z. Xu, Z. Hao, L. Chen, Nickel-doped activated mesoporous carbon microspheres with partially graphitic structure for supercapacitors, Energy Fuels 27 (2013) 1168–1173, https://doi.org/10.1021/ef302028j.
[67] A. Kong, X. Zhu, Z. Han, Y. Yu, Y. Zhang, B. Dong, Y. Shan, Ordered hierarchically micro- and mesoporous Fe-N_x-embedded graphitic architectures as efficient electrocatalysts for oxygen reduction reaction, ACS Catal. 4 (2014) 1793–1800, https://doi.org/10.1021/cs401257j.
[68] J. Yuan, C. Giordano, M. Antonietti, Ionic liquid monomers and polymers as precursors of highly conductive, mesoporous, graphitic carbon nanostructures, Chem. Mater. 22 (2010) 5003–5012, https://doi.org/10.1021/cm1012729.
[69] A.B. Fuertes, T.A. Centeno, Mesoporous carbons with graphitic structures fabricated by using porous silica materials as templates and iron-impregnated polypyrrole as precursor, J. Mater. Chem. 15 (2005) 1079–1083, https://doi.org/10.1039/b416007j.
[70] E. Thompson, A.E. Danks, L. Bourgeois, Z. Schnepp, Iron-catalyzed graphitization of biomass, Green Chem. 17 (2015) 551–556, https://doi.org/10.1039/c4gc01673d.
[71] M. Sevilla, A.B. Fuertes, Catalytic graphitization of templated mesoporous carbons, Carbon 44 (2006) 468–474, https://doi.org/10.1016/j.carbon.2005.08.019. N. Y.
[72] H. Dong, H. Yu, X. Wang, Catalysis kinetics and porous analysis of rolling activated carbon-PTFE air-cathode in microbial fuel cells, Environ. Sci. Technol. 46 (2012) 13009–13015, https://doi.org/10.1021/es303619a.
[73] Z.W. She, J. Kibsgaard, C.F. Dickens, I. Chorkendorff, J.K. Nørskov, T. F. Jaramillo, Combining theory and experiment in electrocatalysis: insights into materials design, Science 355 (2017) eaad4998, https://doi.org/10.1126/science.aad4998.
[74] K. Gong, F. Du, Z. Xia, M. Durstock, L. Dai, Nitrogen-doped carbon nanotube arrays with high electrocatalytic activity for oxygen reduction, Science 323 (2009) 760–764, https://doi.org/10.1126/science.1168049.
[75] S. Hussain, H. Erikson, N. Kongi, A. Sarapuu, J. Solla-Gullón, G. Maia, A. M. Kannan, N. Alonso-Vante, K. Tammeveski, Oxygen reduction reaction on nanostructured Pt-based electrocatalysts: a review, Int. J. Hydrog. Energy 45 (2020) 31775–31797, https://doi.org/10.1016/j.ijhydene.2020.08.215.
[76] R. Zhou, Y. Zheng, M. Jaroniec, S.Z. Qiao, Determination of the electron transfer number for the oxygen reduction reaction: from theory to experiment, ACS Catal. 6 (2016) 4720–4728, https://doi.org/10.1021/acscatal.6b01581.
[77] L. Yang, J. Shui, L. Du, Y. Shao, J. Liu, L. Dai, Z. Hu, Carbon-based metal-free ORR electrocatalysts for fuel cells: past, present, and future, Adv. Mater. 31 (2019), 1804799, https://doi.org/10.1002/adma.201804799.
[78] A. Kulkarni, S. Siahrostami, A. Patel, J.K. Nørskov, Understanding catalytic activity trends in the oxygen reduction reaction, Chem. Rev. 118 (2018) 2302–2312, https://doi.org/10.1021/acs.chemrev.7b00488.
[79] P. Du, X. Xiao, F. Ma, H. Wang, J. Shen, F. Lyu, Y. Chen, J. Lu, Y. Li, Fe,N Co-doped mesoporous carbon nanosheets for oxygen reduction, ACS Appl. Nano Mater. 3 (2020) 5637–5644, https://doi.org/10.1021/acsanm.0c00867.
[80] T. Shinagawa, A.T. Garcia-Esparza, K. Takanabe, Insight on Tafel slopes from a microkinetic analysis of aqueous electrocatalysis for energy conversion, Sci. Rep. 5 (2015) 13801, https://doi.org/10.1038/srep13801.
[81] Z. Zhu, J. Cui, J. Han, S. Wu, H. Sun, W. Liang, A. Li, N-rich mesoporous carbon supported Co-N-C and Fe-N-C catalysts derived from o-phenylenediamine for oxygen reduction reaction, Int. J. Energy Res. 45 (2021) 13531–13544, https://doi.org/10.1002/er.6682.
[82] H.S. Kim, C.H. Lee, J.H. Jang, M.S. Kang, H. Jin, K.S. Lee, S.U. Lee, S.J. Yoo, W. C. Yoo, Single-atom oxygen reduction reaction electrocatalysts of Fe, Si, and N co-doped carbon with 3D interconnected mesoporosity, J. Mater. Chem. A 9 (2021) 4297–4309, https://doi.org/10.1039/d0ta11208a.
[83] C. Hu, L. Dai, Carbon-based metal-free catalysts for electrocatalysis beyond the ORR, Angew. Chem. Int. Ed. 55 (2016) 11736–11758, https://doi.org/10.1002/anie.201509982.
[84] Z. Yang, J. Ren, Z. Zhang, X. Chen, G. Guan, L. Qiu, Y. Zhang, H. Peng, Recent advancement of nanostructured carbon for energy applications, Chem. Rev. 115 (2015) 5159–5223, https://doi.org/10.1021/cr5006217.
[85] N. Daems, X. Sheng, I.F.J. Vankelecom, P.P. Pescarmona, Metal-free doped carbon materials as electrocatalysts for the oxygen reduction reaction, J. Mater. Chem. A 2 (2014) 4085–4110, https://doi.org/10.1039/c3ta14043a.
[86] X. Sheng, N. Daems, B. Geboes, M. Kurttepeli, S. Bals, T. Breugelmans, A. Hubin, I.F.J. Vankelecom, P.P. Pescarmona, N-doped ordered mesoporous carbons prepared by a two-step nanocasting strategy as highly active and selective electrocatalysts for the reduction of O_2 to H_2O_2, Appl. Catal. B Environ. 176–177 (2015) 212–224, https://doi.org/10.1016/j.apcatb.2015.03.049.
[87] Y. Pang, K. Wang, H. Xie, Y. Sun, M.M. Titirici, G.L. Chai, Mesoporous carbon hollow spheres as efficient electrocatalysts for oxygen reduction to hydrogen peroxide in neutral electrolytes, ACS Catal. 10 (2020) 7434–7442, https://doi.org/10.1021/acscatal.0c00584.
[88] D.H. Kwak, S.B. Han, D.H. Kim, J.Y. Park, K.B. Ma, J.E. Won, M.C. Kim, S. H. Moon, K.W. Park, Investigation of the durability of Fe/N-doped mesoporous carbon nanostructure as a non-precious metal catalyst for oxygen reduction reaction in acid medium, Carbon 140 (2018) 189–200, https://doi.org/10.1016/j.carbon.2018.08.053. N. Y.
[89] J. Lilloja, E. Kibena-Põldsepp, M. Merisalu, P. Rauwel, L. Matisen, A. Niilisk, E.S. F. Cardoso, G. Maia, V. Sammelselg, K. Tammeveski, An oxygen reduction study of graphene-based nanomaterials of different origin, Catalysts 6 (2016) 108, https://doi.org/10.3390/catal6070108.
[90] J. Zhang, Z. Zhao, Z. Xia, L. Dai, A metal-free bifunctional electrocatalyst for oxygen reduction and oxygen evolution reactions, Nat. Nanotechnol. 10 (2015) 444–452, https://doi.org/10.1038/nnano.2015.48.
[91] W. Yang, T.P. Fellinger, M. Antonietti, Efficient metal-free oxygen reduction in alkaline medium on high-surface-area mesoporous nitrogen-doped carbons made from ionic liquids and nucleobases, J. Am. Chem. Soc. 133 (2011) 206–209, https://doi.org/10.1021/ja108039j.
[92] K. Wan, G.F. Long, M.Y. Liu, L. Du, Z.X. Liang, P. Tsiakaras, Nitrogen-doped ordered mesoporous carbon: synthesis and active sites for electrocatalysis of oxygen reduction reaction, Appl. Catal. B Environ. 165 (2015) 566–571, https://doi.org/10.1016/j.apcatb.2014.10.054.
[93] G.A. Ferrero, K. Preuss, A.B. Fuertes, M. Sevilla, M.M. Titirici, The influence of pore size distribution on the oxygen reduction reaction performance in nitrogen doped carbon microspheres, J. Mater. Chem. A 4 (2016) 2581–2589, https://doi.org/10.1039/c5ta10063a.

[94] J. Quílez-Bermejo, E. Morallón, D. Cazorla-Amorós, Polyaniline-derived N-doped ordered mesoporous carbon thin films: efficient catalysts towards oxygen reduction reaction, Polymers 12 (2020) 1–17, https://doi.org/10.3390/polym12102382 (Basel).
[95] Z. Zhang, J. Sun, M. Dou, J. Ji, F. Wang, Nitrogen and phosphorus codoped mesoporous carbon derived from polypyrrole as superior metal-free electrocatalyst toward the oxygen reduction reaction, ACS Appl. Mater. Interfaces 9 (2017) 16236–16242, https://doi.org/10.1021/acsami.7b03375.
[96] X. Xia, C.F. Cheng, Y. Zhu, B.D. Vogt, Ultrafast microwave-assisted synthesis of highly nitrogen-doped ordered mesoporous carbon, Microporous Mesoporous Mater. 310 (2021), 110639, https://doi.org/10.1016/j.micromeso.2020.110639.
[97] X. Liu, S. Li, L. Liu, Z. Wang, Facile pyrolysis approach of folic acid-derived high graphite N-doped porous carbon materials for the oxygen reduction reaction, New J. Chem. 45 (2021) 5949–5957, https://doi.org/10.1039/d0nj06174c.
[98] J. Min, X. Xu, J.J. Koh, J. Gong, X. Chen, J. Azadmanjiri, F. Zhang, X. Wen, C. He, Branched poly(l-lysine)-derived nitrogen-containing porous carbon flake as the metal-free electrocatalyst toward efficient oxygen reduction reaction, ACS Appl. Energy Mater. 4 (2021) 3317–3326, https://doi.org/10.1021/acsaem.0c03070.
[99] W. Zhang, J. Qi, P. Bai, H. Wang, L. Xu, High-level nitrogen-doped, micro/mesoporous carbon as an efficient metal-free electrocatalyst for the oxygen reduction reaction: optimizing the reaction surface area by a solvent-free mechanochemical method, New J. Chem. 43 (2019) 10878–10886, https://doi.org/10.1039/c9nj01997a.
[100] T. Zhou, Y. Zhou, R. Ma, Z. Zhou, G. Liu, Q. Liu, Y. Zhu, J. Wang, Nitrogen-doped hollow mesoporous carbon spheres as a highly active and stable metal-free electrocatalyst for oxygen reduction, Carbon 114 (2017) 177–186, https://doi.org/10.1016/j.carbon.2016.12.011. N. Y.
[101] X. Zhang, X. Xu, S. Yao, C. Hao, C. Pan, X. Xiang, Z.Q. Tian, P.K. Shen, Z. Shao, S. P. Jiang, Boosting electrocatalytic activity of single atom catalysts supported on nitrogen-doped carbon through N coordination environment engineering, Small 18 (2022), 2105329, https://doi.org/10.1002/smll.202105329.
[102] W. Wei, H. Liang, K. Parvez, X. Zhuang, X. Feng, K. Müllen, Nitrogen-doped carbon nanosheets with size-defined mesopores as highly efficient metal-free catalyst for the oxygen reduction reaction, Angew. Chem. Int. Ed. 53 (2014) 1570–1574, https://doi.org/10.1002/anie.201307319.
[103] J. Tang, J. Liu, C. Li, Y. Li, M.O. Tade, S. Dai, Y. Yamauchi, Synthesis of nitrogen-doped mesoporous carbon spheres with extra-large pores through assembly of diblock copolymer micelles, Angew. Chem. Int. Ed. 54 (2015) 588–593, https://doi.org/10.1002/anie.201407629.
[104] U.B. Nasini, V. GopalBairi, S. KumarRamasahayam, S.E. Bourdo, T. Viswanathan, A.U. Shaikh, Oxygen reduction reaction studies of phosphorus and nitrogen co-doped mesoporous carbon synthesized via microwave technique, ChemElectroChem 1 (2014) 573–579, https://doi.org/10.1002/celc.201300047.
[105] A. Chen, Q. Yi, K. Sheng, Y. Wang, J. Chen, K. Xiang, H. Nie, X. Zhou, Nitrogen and phosphorus co-doped ultrathin carbon nanosheets as superior cathode catalysts for Zn-air batteries, Sustain. Energy Fuels 5 (2021) 2458–2468, https://doi.org/10.1039/d1se00275a.
[106] Y. Zan, Z. Zhang, B. Zhu, M. Dou, F. Wang, Ultrathin two-dimensional phosphorus and nitrogen Co-doped carbon nanosheet as efficient oxygen reduction electrocatalyst, Carbon 174 (2021) 404–412, https://doi.org/10.1016/j.carbon.2020.12.058. N. Y.
[107] M. Li, C. Wang, S. Hu, H. Wu, C. Feng, Y. Zhang, Nitrogen, phosphorus co-doped mesoporous carbon materials as efficient catalysts for oxygen reduction reaction, Ionics 25 (2019) 4295–4303, https://doi.org/10.1007/s11581-019-02976-9 (Kiel).
[108] K. Lv, H. Zhang, S. Chen, Nitrogen and phosphorus co-doped carbon modified activated carbon as an efficient oxygen reduction catalyst for microbial fuel cells, RSC Adv. 8 (2018) 848–855, https://doi.org/10.1039/c7ra12907f.
[109] C. Deng, H. Zhong, X. Li, L. Yao, H. Zhang, A highly efficient electrocatalyst for oxygen reduction reaction: phosphorus and nitrogen co-doped hierarchically ordered porous carbon derived from an iron-functionalized polymer, Nanoscale 8 (2016) 1580–1587, https://doi.org/10.1039/c5nr06749a.
[110] L. Samiee, S.S. Hassani, N and s co-doped ordered mesoporous carbon: an efficient electrocatalyst for oxygen reduction reaction in microbial fuel cells, Curr. Nanosci. 16 (2020) 625–638, https://doi.org/10.2174/1573413716666191231094731.
[111] S. Son, D. Lim, D. Nam, J. Kim, S.E. Shim, S.H. Baeck, N, S-doped nanocarbon derived from ZIF-8 as a highly efficient and durable electro-catalyst for oxygen reduction reaction, J. Solid State Chem. 274 (2019) 237–242, https://doi.org/10.1016/j.jssc.2019.03.036.
[112] Y. Zan, Z. Zhang, M. Dou, F. Wang, Enhancement mechanism of sulfur dopants on the catalytic activity of N and P co-doped three-dimensional hierarchically porous carbon as a metal-free oxygen reduction electrocatalyst, Catal. Sci. Technol. 9 (2019) 5906–5914, https://doi.org/10.1039/c9cy01387c.
[113] T. Oh, M. Kim, D. Park, J. Kim, Synergistic interaction and controllable active sites of nitrogen and sulfur co-doping into mesoporous carbon sphere for high performance oxygen reduction electrocatalysts, Appl. Surf. Sci. 440 (2018) 627–636, https://doi.org/10.1016/j.apsusc.2018.01.186.
[114] H. Zhao, Y.P. Zhu, L. Ge, Z.Y. Yuan, Nitrogen and sulfur co-doped mesoporous hollow carbon microspheres for highly efficient oxygen reduction electrocatalysts, Int. J. Hydrog. Energy 42 (2017) 19010–19018, https://doi.org/10.1016/j.ijhydene.2017.06.172.
[115] Y. Hua, T. Jiang, K. Wang, M. Wu, S. Song, Y. Wang, P. Tsiakaras, Efficient Pt-free electrocatalyst for oxygen reduction reaction: highly ordered mesoporous N and S co-doped carbon with saccharin as single-source molecular precursor, Appl. Catal. B Environ. 194 (2016) 202–208, https://doi.org/10.1016/j.apcatb.2016.04.056.
[116] V. Perazzolo, E. Grądzka, C. Durante, R. Pilot, N. Vicentini, G.A. Rizzi, G. Granozzi, A. Gennaro, Chemical and electrochemical stability of nitrogen and sulphur doped mesoporous carbons, Electrochim. Acta 197 (2016) 251–262, https://doi.org/10.1016/j.electacta.2016.02.025.
[117] J. Shi, X. Zhou, P. Xu, J. Qiao, Z. Chen, Y. Liu, Nitrogen and sulfur co-doped mesoporous carbon materials as highly efficient electrocatalysts for oxygen reduction reaction, Electrochim. Acta 145 (2014) 259–269, https://doi.org/10.1016/j.electacta.2014.08.091.
[118] A.M. Al-Enizi, Waste cigarette butt-derived B, N doped bifunctional hierarchical mesoporous carbon for supercapacitor and oxygen reduction reaction, Colloids Surf. A Physicochem. Eng. Asp. 643 (2022), 128775, https://doi.org/10.1016/j.colsurfa.2022.128775.
[119] V. Duraisamy, S.M.S. Kumar, Study of the secondary heteroatoms doping on nitrogen-doped carbon and their oxygen reduction reaction performance evaluation, ChemistrySelect 6 (2021) 11887–11899, https://doi.org/10.1002/slct.202103506.
[120] U. Byambasuren, Y. Jeon, D. Altansukh, Y.G. Shul, Doping effect of boron and phosphorus on nitrogen-based mesoporous carbons as electrocatalysts for oxygen reduction reaction in acid media, J. Solid State Electrochem. 20 (2016) 645–655, https://doi.org/10.1007/s10008-015-3074-6.
[121] I.A. Pašti, N.M. Gavrilov, A.S. Dobrota, M. Momčilović, M. Stojmenović, A. Topalov, D.M. Stanković, B. Babić, G. Ćirić-Marjanović, S.V. Mentus, The effects of a low-level boron, phosphorus, and nitrogen doping on the oxygen reduction activity of ordered mesoporous carbons, Electrocatalysis 6 (2015) 498–511, https://doi.org/10.1007/s12678-015-0271-0.
[122] X. Bo, L. Guo, Ordered mesoporous boron-doped carbons as metal-free electrocatalysts for the oxygen reduction reaction in alkaline solution, Phys. Chem. Chem. Phys. 15 (2013) 2459–2465, https://doi.org/10.1039/c2cp43541a.
[123] G. Zhao, L. Shi, J. Xu, X. Yan, T.S. Zhao, Role of phosphorus in nitrogen, phosphorus dual-doped ordered mesoporous carbon electrocatalyst for oxygen reduction reaction in alkaline media, Int. J. Hydrog. Energy 43 (2018) 1470–1478, https://doi.org/10.1016/j.ijhydene.2017.11.165.
[124] G. Lin, R. Ma, Y. Zhou, Q. Liu, X. Dong, J. Wang, KOH activation of biomass-derived nitrogen-doped carbons for supercapacitor and electrocatalytic oxygen reduction, Electrochim. Acta 261 (2018) 49–57, https://doi.org/10.1016/j.electacta.2017.12.107.
[125] C. Xu, Z. Li, L. Yang, L. Hu, W. Wang, J. Huang, H. Zhou, L. Chen, Z. Hou, Dopant–free edge–rich mesoporous carbon: understanding the role of intrinsic carbon defects towards oxygen reduction reaction, J. Electroanal. Chem. 923 (2022), https://doi.org/10.1016/j.jelechem.2022.116826.
[126] D. Yan, Y. Li, J. Huo, R. Chen, L. Dai, S. Wang, Defect chemistry of nonprecious-metal electrocatalysts for oxygen reactions, Adv. Mater. 29 (2017), 1606459, https://doi.org/10.1002/adma.201606459.
[127] G. Zhong, Z. Meng, M. Xu, H. Xie, S. Xu, X. Fu, W. Liao, S. Zheng, Y. Xu, Self-nitrogen-doped porous carbon prepared via pyrolysis of grass-blade without additive for oxygen reduction reaction, Diam. Relat. Mater. 121 (2022), 108742, https://doi.org/10.1016/j.diamond.2021.108742.
[128] V. Duraisamy, R. Krishnan, S.M. Senthil Kumar, N-doped hollow mesoporous carbon nanospheres for oxygen reduction reaction in alkaline media, ACS Appl. Nano Mater. 3 (2020) 8875–8887, https://doi.org/10.1021/acsanm.0c01639.
[129] Z. Wu, R. Liu, J. Wang, J. Zhu, W. Xiao, C. Xuan, W. Lei, D. Wang, Nitrogen and sulfur co-doping of 3D hollow-structured carbon spheres as an efficient and stable metal free catalyst for the oxygen reduction reaction, Nanoscale 8 (2016) 19086–19092, https://doi.org/10.1039/c6nr06817k.
[130] Y. Zheng, S. Chen, K.A.I. Zhang, J. Guan, X. Yu, W. Peng, H. Song, J. Zhu, J. Xu, X. Fan, C. Zhang, T. Liu, Template-free construction of hollow mesoporous carbon spheres from a covalent triazine framework for enhanced oxygen electroreduction, J. Colloid Interface Sci. 608 (2022) 3168–3177, https://doi.org/10.1016/j.jcis.2021.11.048.
[131] H. Rong, T. Zhan, Y. Sun, Y. Wen, X. Liu, H. Teng, ZIF-8 derived nitrogen, phosphorus and sulfur tri-doped mesoporous carbon for boosting electrocatalysis to oxygen reduction in universal pH range, Electrochim. Acta 318 (2019) 783–793, https://doi.org/10.1016/j.electacta.2019.06.122.
[132] S. Jiang, C. Li, J. Zhang, Q. Li, H. Xu, F. Xu, Y. Mai, Block copolymer self-assembly guided synthesis of mesoporous carbons with in-plane holey pores for efficient oxygen reduction reaction, Macromol. Rapid Commun. 43 (2022), 2100884, https://doi.org/10.1002/marc.202100884.
[133] J. Lilloja, E. Kibena-Põldsepp, A. Sarapuu, M. Käärik, J. Kozlova, P. Paiste, A. Kikas, A. Treshchalov, J. Leis, A. Tamm, V. Kisand, S. Holdcroft, K. Tammeveski, Transition metal and nitrogen-doped mesoporous carbons as cathode catalysts for anion-exchange membrane fuel cells, Appl. Catal. B Environ. 306 (2022), 121113, https://doi.org/10.1016/j.apcatb.2022.121113.
[134] J. Lilloja, M. Mooste, E. Kibena-Põldsepp, A. Sarapuu, B. Zulevi, A. Kikas, H. M. Piirsoo, A. Tamm, V. Kisand, S. Holdcroft, A. Serov, K. Tammeveski, Mesoporous iron-nitrogen co-doped carbon material as cathode catalyst for the anion exchange membrane fuel cell, J. Power Sources Adv. 8 (2021), 100052, https://doi.org/10.1016/j.powera.2021.100052.
[135] C. Shu, Q. Tan, C. Deng, W. Du, Z. Gan, Y. Liu, C. Fan, H. Jin, W. Tang, X.D. Yang, X. Yang, Y. Wu, Hierarchically mesoporous carbon spheres coated with a single atomic Fe–N–C layer for balancing activity and mass transfer in fuel cells, Carbon Energy 4 (2022) 1–11, https://doi.org/10.1002/cey2.136.
[136] S. Liu, Z. Yang, M. Li, W. Lv, L. Liu, Y. Wang, X. Chen, X. Zhao, P. Zhu, G. Wang, Facile synthesis of 3D hierarchical mesoporous Fe-C-N catalysts as efficient electrocatalysts for oxygen reduction reaction, Int. J. Hydrog. Energy 43 (2018) 5163–5174, https://doi.org/10.1016/j.ijhydene.2018.01.151.

[137] X. Zhang, L. Wu, Polyvinyl pyrrolidone regulated Co, N co-doped porous carbon for oxygen reduction reaction, Ionics 28 (2022) 3435–3443, https://doi.org/10.1007/s11581-022-04581-9 (Kiel).
[138] W. Li, B. Liu, D. Liu, P. Guo, J. Liu, R. Wang, Y. Guo, X. Tu, H. Pan, D. Sun, F. Fang, R. Wu, Alloying Co species into ordered and interconnected macroporous carbon polyhedra for efficient oxygen reduction reaction in rechargeable zinc–air batteries, Adv. Mater. 34 (2022), 2109605, https://doi.org/10.1002/adma.202109605.
[139] X. Wei, D. Zheng, M. Zhao, H. Chen, X. Fan, B. Gao, L. Gu, Y. Guo, J. Qin, J. Wei, Y. Zhao, G. Zhang, Cross-linked polyphosphazene hollow nanosphere-derived N/P-doped porous carbon with single nonprecious metal atoms for the oxygen reduction reaction, Angew. Chem. Int. Ed. 59 (2020) 14639–14646, https://doi.org/10.1002/anie.202006175.
[140] H. Tang, Y. Zeng, D. Liu, D. Qu, J. Luo, K. Binnemans, D.E. De Vos, J. Fransaer, D. Qu, S.G. Sun, Dual-doped mesoporous carbon synthesized by a novel nanocasting method with superior catalytic activity for oxygen reduction, Nano Energy 26 (2016) 131–138, https://doi.org/10.1016/j.nanoen.2016.05.015.
[141] G.L. Li, Z.F. Lu, X. Wang, S. Cao, C. Hao, Rational construction of atomically dispersed Mn-N_x embedded in mesoporous N-doped amorphous carbon for efficient oxygen reduction reaction in Zn-Air batteries, ACS Sustain. Chem. Eng. 10 (2022) 224–233, https://doi.org/10.1021/acssuschemeng.1c05882.
[142] A. Byeon, J. Cho, J.M. Kim, K.H. Chae, H.Y. Park, S.W. Hong, H.C. Ham, S.W. Lee, K.R. Yoon, J.Y. Kim, High-yield electrochemical hydrogen peroxide production from an enhanced two-electron oxygen reduction pathway by mesoporous nitrogen-doped carbon and manganese hybrid electrocatalysts, Nanoscale Horiz. 5 (2020) 832–838, https://doi.org/10.1039/c9nh00783k.
[143] S. Liu, Z. Yang, M. Li, L. Liu, Y. Wang, W. Lv, Z. Qin, X. Zhao, P. Zhu, G. Wang, FeS-decorated hierarchical porous N, S-dual-doped carbon derived from silica-ionogel as an efficient catalyst for oxygen reduction reaction in alkaline media, Electrochim. Acta 265 (2018) 221–231, https://doi.org/10.1016/j.electacta.2018.01.195.
[144] J. Masa, A. Zhao, X. Wei, M. Muhler, W. Schuhmann, Metal-free catalysts for oxygen reduction in alkaline electrolytes: influence of the presence of Co, Fe, Mn and Ni inclusions, Electrochim. Acta 128 (2014) 271–278, https://doi.org/10.1016/j.electacta.2013.11.026.
[145] C. Guo, Y. Li, W. Liao, Y. Liu, Z. Li, L. Sun, C. Chen, J. Zhang, Y. Si, L. Li, Boosting the oxygen reduction activity of a three-dimensional network Co-N-C electrocatalyst via space-confined control of nitrogen-doping efficiency and the molecular-level coordination effect, J. Mater. Chem. A 6 (2018) 13050–13061, https://doi.org/10.1039/c8ta03759k.
[146] V. Nallathambi, J.W. Lee, S.P. Kumaraguru, G. Wu, B.N. Popov, Development of high performance carbon composite catalyst for oxygen reduction reaction in PEM proton exchange membrane fuel cells, J. Power Sources 183 (2008) 34–42, https://doi.org/10.1016/j.jpowsour.2008.05.020.
[147] P.H. Matter, E. Wang, M. Arias, E.J. Biddinger, U.S. Ozkan, Oxygen reduction reaction catalysts prepared from acetonitrile pyrolysis over alumina-supported metal particles, J. Phys. Chem. B 110 (2006) 18374–18384, https://doi.org/10.1021/jp062206d.
[148] Y. Li, W. Zhou, H. Wang, L. Xie, Y. Liang, F. Wei, J.C. Idrobo, S.J. Pennycook, H. Dai, An oxygen reduction electrocatalyst based on carbon nanotube-graphene complexes, Nat. Nanotechnol. 7 (2012) 394–400, https://doi.org/10.1038/nnano.2012.72.
[149] F. Jaouen, M. Lefèvre, J.P. Dodelet, M. Cai, Heat-treated Fe/N/C catalysts for O_2 electroreduction: are active sites hosted in micropores? J. Phys. Chem. B 110 (2006) 5553–5558, https://doi.org/10.1021/jp057135h.
[150] M. He, S. Song, P. Wang, Z. Fang, W. Wang, X. Yuan, C. Li, H. Li, W. Song, D. Luo, Z. Li, Carbon doped cobalt nanoparticles stabilized by carbon shell for highly efficient and stable oxygen reduction reaction, Carbon 196 (2022) 483–492, https://doi.org/10.1016/j.carbon.2022.05.019. N. Y.
[151] J. Li, W. Xia, J. Tang, H. Tan, J. Wang, Y.V. Kaneti, Y. Bando, T. Wang, J. He, Y. Yamauchi, MOF nanoleaves as new sacrificial templates for the fabrication of nanoporous Co-N:X/C electrocatalysts for oxygen reduction, Nanoscale Horiz. 4 (2019) 1006–1013, https://doi.org/10.1039/c9nh00095j.
[152] L. Yang, S. Feng, G. Xu, B. Wei, L. Zhang, Electrospun MOF-based FeCo nanoparticles embedded in nitrogen-doped mesoporous carbon nanofibers as an efficient bifunctional catalyst for oxygen reduction and oxygen evolution reactions in zinc-air batteries, ACS Sustain. Chem. Eng. 7 (2019) 5462–5475, https://doi.org/10.1021/acssuschemeng.8b06624.
[153] V. Jose, A. Jayakumar, J.M. Lee, Bimetal/metal oxide encapsulated in graphitic nitrogen doped mesoporous carbon networks for enhanced oxygen electrocatalysis, ChemElectroChem 6 (2019) 1485–1491, https://doi.org/10.1002/celc.201801508.
[154] F. Zhang, Y. Chen, Y. Liu, X. Liu, S. Gao, Template-assisted polymerization-pyrolysis derived mesoporous carbon anchored with Fe/Fe_3C and Fe−NX species as efficient oxygen reduction catalysts for Zn-air battery, Int. J. Hydrog. Energy 46 (2021) 37895–37906, https://doi.org/10.1016/j.ijhydene.2021.09.040.
[155] K. Wang, H. Chen, X. Zhang, Y. Tong, S. Song, P. Tsiakaras, Y. Wang, Iron oxide@graphitic carbon core-shell nanoparticles embedded in ordered mesoporous N-doped carbon matrix as an efficient cathode catalyst for PEMFC, Appl. Catal. B Environ. 264 (2020), 118468, https://doi.org/10.1016/j.apcatb.2019.118468.
[156] K. Huang, Y. Xu, Y. Song, R. Wang, H. Wei, Y. Long, M. Lei, H. Tang, J. Guo, H. Wu, $NiPS_3$ quantum sheets modified nitrogen-doped mesoporous carbon with boosted bifunctional oxygen electrocatalytic performance, J. Mater. Sci. Technol. 65 (2021) 1–6, https://doi.org/10.1016/j.jmst.2020.04.065.
[157] H. Yuan, J. Li, W. Yang, Z. Zhuang, Y. Zhao, L. He, L. Xu, X. Liao, R. Zhu, L. Mai, Oxygen vacancy-determined highly efficient oxygen reduction in $NiCo_2O_4$/hollow carbon spheres, ACS Appl. Mater. Interfaces 10 (2018) 16410–16417, https://doi.org/10.1021/acsami.8b01209.
[158] R. Zhang, K. Huang, D. Wang, N. Hussain, A. Zhang, H. Wei, G. Ou, W. Zhao, C. Zhang, H. Wu, Ultrafine Fe/Fe_3C nanoparticles on nitrogen-doped mesoporous carbon by low-temperature synthesis for highly efficient oxygen reduction, Electrochim. Acta 313 (2019) 255–260, https://doi.org/10.1016/j.electacta.2019.05.024.
[159] G.H. An, E.H. Lee, H.J. Ahn, Well-dispersed iron nanoparticles exposed within nitrogen-doped mesoporous carbon nanofibers by hydrogen-activation for oxygen-reduction reaction, J. Alloy. Compd. 682 (2016) 746–752, https://doi.org/10.1016/j.jallcom.2016.05.033.
[160] Y. Deng, X. Tian, G. Shen, Y. Gao, C. Lin, L. Ling, F. Cheng, S. Liao, S. Zhang, Coupling hollow Fe_3O_4 nanoparticles with oxygen vacancy on mesoporous carbon as a high-efficiency ORR electrocatalyst for Zn-air battery, J. Colloid Interface Sci. 567 (2020) 410–418, https://doi.org/10.1016/j.jcis.2020.02.013.
[161] B. Wang, Y. Ye, L. Xu, Y. Quan, W. Wei, W. Zhu, H. Li, J. Xia, Space-confined yolk-shell construction of Fe_3O_4 nanoparticles inside N-doped hollow mesoporous carbon spheres as bifunctional electrocatalysts for long-term rechargeable zinc–air batteries, Adv. Funct. Mater. (2020), 2005834, https://doi.org/10.1002/adfm.202005834.
[162] Z. Xiao, F. Hou, Y. Li, R. Zhang, G. Shen, L. Wang, X. Zhang, Q. Wang, G. Li, Confinement of Fe_2O_3 nanoparticles in the shell of N-doped carbon hollow microsphere for efficient oxygen reduction reaction, Chem. Eng. Sci. 207 (2019) 235–246, https://doi.org/10.1016/j.ces.2019.06.029.
[163] Y. Zang, H. Zhang, X. Zhang, R. Liu, S. Liu, G. Wang, Y. Zhang, H. Zhao, Fe/Fe_2O_3 nanoparticles anchored on Fe-N-doped carbon nanosheets as bifunctional oxygen electrocatalysts for rechargeable zinc-air batteries, Nano Res. 9 (2016) 2123–2137, https://doi.org/10.1007/s12274-016-1102-1.
[164] A. Samanta, C.R. Raj, Bifunctional nitrogen-doped hybrid catalyst based on onion-like carbon and graphitic carbon encapsulated transition metal alloy nanostructure for rechargeable zinc-air battery, J. Power Sources 455 (2020), 227975, https://doi.org/10.1016/j.jpowsour.2020.227975.
[165] S.M. Alshehri, A.N. Alhabarah, J. Ahmed, M. Naushad, T. Ahamad, An efficient and cost-effective tri-functional electrocatalyst based on cobalt ferrite embedded nitrogen doped carbon, J. Colloid Interface Sci. 514 (2018) 1–9, https://doi.org/10.1016/j.jcis.2017.12.020.
[166] P. Li, R. Ma, Y. Zhou, Y. Chen, Z. Zhou, G. Liu, Q. Liu, G. Peng, Z. Liang, J. Wang, *In situ* growth of spinel $CoFe_2O_4$ nanoparticles on rod-like ordered mesoporous carbon for bifunctional electrocatalysis of both oxygen reduction and oxygen evolution, J. Mater. Chem. A 3 (2015) 15598–15606, https://doi.org/10.1039/c5ta02625c.
[167] H. Wang, X. Qiu, W. Wang, L. Jiang, H. Liu, Iron sulfide nanoparticles embedded into a nitrogen and sulfur co-doped carbon sphere as a highly active oxygen reduction electrocatalyst, Front. Chem. 7 (2019) 855, https://doi.org/10.3389/fchem.2019.00855.
[168] M.M. Weng, D.J. Liu, X.Q. He, T. Asefa, Fe_3C nanoparticles-loaded 3D nanoporous N-doped carbon: a highly efficient electrocatalyst for oxygen reduction in alkaline media, Int. J. Hydrog. Energy 44 (2019) 21506–21517, https://doi.org/10.1016/j.ijhydene.2019.06.062.
[169] X. Xin, H. Qin, H.P. Cong, S.H. Yu, Templating synthesis of mesoporous Fe_3C-encapsulated Fe-N-doped carbon hollow nanospindles for electrocatalysis, Langmuir 34 (2018) 4952–4961, https://doi.org/10.1021/acs.langmuir.8b00548.
[170] H. Jiang, Y. Yao, Y. Zhu, Y. Liu, Y. Su, X. Yang, C. Li, Iron carbide nanoparticles encapsulated in mesoporous Fe-N-doped graphene-like carbon hybrids as efficient bifunctional oxygen electrocatalysts, ACS Appl. Mater. Interfaces 7 (2015) 21511–21520, https://doi.org/10.1021/acsami.5b06708.
[171] Z.Y. Wu, X.X. Xu, B.C. Hu, H.W. Liang, Y. Lin, L.F. Chen, S.H. Yu, Iron carbide nanoparticles encapsulated in mesoporous Fe-N-doped carbon nanofibers for efficient electrocatalysis, Angew. Chem. Int. Ed. 54 (2015) 8179–8183A, https://doi.org/10.1002/anie.201502173.
[172] J. Gautam, D.T. Tran, T.I. Singh, N.H. Kim, J.H. Lee, Mesoporous iron sulfide nanoparticles anchored graphene sheet as an efficient and durable catalyst for oxygen reduction reaction, J. Power Sources 427 (2019) 91–100, https://doi.org/10.1016/j.jpowsour.2019.04.075.
[173] G.L. Li, L.F. Yuan, W.W. Chen, B.B. Yang, C.D. Liu, G.C. Cheng, X.C. Xu, C. Hao, Efficient hierarchically synthesized Fe_2P nanoparticles embedded in an N,P-doped mesoporous carbon catalyst for the oxygen reduction reaction, New J. Chem. 42 (2018) 9488–9495, https://doi.org/10.1039/c8nj00380g.
[174] X. Xu, C. Shi, R. Chen, T. Chen, Iron phosphide nanocrystals decorated *in situ* on heteroatom-doped mesoporous carbon nanosheets used for an efficient oxygen reduction reaction in both alkaline and acidic media, RSC Adv. 7 (2017) 22263–22269, https://doi.org/10.1039/c7ra02349a.
[175] M. Li, X. Bo, Y. Zhang, C. Han, A. Nsabimana, L. Guo, Cobalt and nitrogen co-embedded onion-like mesoporous carbon vesicles as efficient catalysts for oxygen reduction reaction, J. Mater. Chem. A 2 (2014) 11672–11682, https://doi.org/10.1039/c4ta01078g.
[176] H. Han, Z. Bai, X. Wang, S. Chao, J. Liu, Q. Kong, X. Yang, L. Yang, Highly dispersed Co nanoparticles inlayed in S, N-doped hierarchical carbon nanoprisms derived from Co-MOFs as efficient electrocatalysts for oxygen reduction reaction, Catal. Today 318 (2018) 126–131, https://doi.org/10.1016/j.cattod.2018.03.032.
[177] L. Pan, G. Chen, G. Chen, D. Chen, Electrospun cobalt nanoparticles embedded in pyrrole doped hollow mesoporous carbon nanofibers as efficient and durable oxygen electrocatalysts for rechargeable zinc-air battery, Diam. Relat. Mater. 127 (2022), 109178, https://doi.org/10.1016/j.diamond.2022.109178.

[178] Y. Wang, Y. Zhou, Y. Feng, X.Y. Yu, Synergistic electronic and pore structure modulation in open carbon nanocages enabling efficient electrocatalytic production of H_2O_2 in acidic medium, Adv. Funct. Mater. 32 (2022), 2110734, https://doi.org/10.1002/adfm.202110734.
[179] C. Xu, Z. Lin, D. Zhao, Y. Sun, Y. Zhong, J. Ning, C. Zheng, Z. Zhang, Y. Hu, Facile *in situ* fabrication of Co nanoparticles embedded in 3D N-enriched mesoporous carbon foam electrocatalyst with enhanced activity and stability toward oxygen reduction reaction, J. Mater. Sci. 54 (2019) 5412–5423, https://doi.org/10.1007/s10853-018-03255-0.
[180] V.M. Bau, X. Bo, L. Guo, Nitrogen-doped cobalt nanoparticles/nitrogen-doped plate-like ordered mesoporous carbons composites as noble-metal free electrocatalysts for oxygen reduction reaction, J. Energy Chem. 26 (2017) 63–71, https://doi.org/10.1016/j.jechem.2016.07.005.
[181] S. Zhao, J. Yang, M. Han, X. Wang, Y. Lin, R. Yang, D. Xu, N. Shi, Q. Wang, M. Yang, Z. Dai, J. Bao, Synergistically enhanced oxygen reduction electrocatalysis by atomically dispersed and nanoscaled Co species in three-dimensional mesoporous Co, N-codoped carbon nanosheets network, Appl. Catal. B Environ. 260 (2020), 118207, https://doi.org/10.1016/j.apcatb.2019.118207.
[182] X. Wan, X. Guo, M. Duan, J. Shi, S. Liu, J. Zhang, Y. Liu, X. Zheng, Q. Kong, Ultrafine CoO nanoparticles and Co-N-C lamellae supported on mesoporous carbon for efficient electrocatalysis of oxygen reduction in zinc-air batteries, Electrochim. Acta 394 (2021), 139135, https://doi.org/10.1016/j.electacta.2021.139135.
[183] W. Hu, Q. Wang, S. Wu, Y. Huang, Facile one-pot synthesis of a nitrogen-doped mesoporous carbon architecture with cobalt oxides encapsulated in graphitic layers as a robust bicatalyst for oxygen reduction and evolution reactions, J. Mater. Chem. A 4 (2016) 16920–16927, https://doi.org/10.1039/c6ta08103g.
[184] P. Li, R. Ma, Y. Zhou, Y. Chen, Q. Liu, G. Peng, J. Wang, The direct growth of highly dispersed CoO nanoparticles on mesoporous carbon as a high-performance electrocatalyst for the oxygen reduction reaction, RSC Adv. 6 (2016) 70763–70769, https://doi.org/10.1039/c6ra14394f.
[185] G. Xu, G.C. Xu, J.J. Ban, L. Zhang, H. Lin, C.L. Qi, Z.P. Sun, D.Z. Jia, Cobalt and cobalt oxides N-codoped porous carbon derived from metal-organic framework as bifunctional catalyst for oxygen reduction and oxygen evolution reactions, J. Colloid Interface Sci. 521 (2018) 141–149, https://doi.org/10.1016/j.jcis.2018.03.036.
[186] Y. Liu, T. Zhang, Y.E. Duan, X. Dai, Q. Tan, Y. Chen, Y. Liu, N, O-codoped carbon spheres with uniform mesoporous entangled Co_3O_4 nanoparticles as a highly efficient electrocatalyst for oxygen reduction in a Zn-air battery, J. Colloid Interface Sci. 604 (2021) 746–756, https://doi.org/10.1016/j.jcis.2021.07.040.
[187] B. Wang, L. Xu, G. Liu, P. Zhang, W. Zhu, J. Xia, H. Li, Biomass willow catkin-derived Co_3O_4/N-doped hollow hierarchical porous carbon microtubes as an effective tri-functional electrocatalyst, J. Mater. Chem. A 5 (2017) 20170–20179, https://doi.org/10.1039/c7ta05002j.
[188] W. Liu, Z. Zhou, Z. Li, Y. Yang, J. Zhao, Y. Zhu, W. Miao, Cobalt phosphide embedded N-doped carbon nanopolyhedral as an efficient cathode electrocatalyst in microbial fuel cells, J. Environ. Chem. Eng. 9 (2021), 139135, https://doi.org/10.1016/j.jece.2020.104582.
[189] B. Liang, C. Ren, Y. Zhao, K. Li, C. Lv, Nitrogenous mesoporous carbon coated with Co/Cu nanoparticles modified activated carbon as air cathode catalyst for microbial fuel cell, J. Electroanal. Chem. 860 (2020), 113904, https://doi.org/10.1016/j.jelechem.2020.113904.
[190] Z. Shang, Z. Chen, Z. Zhang, J. Yu, S. Tan, F. Ciucci, Z. Shao, H. Lei, D. Chen, CoFe nanoalloy particles encapsulated in nitrogen-doped carbon layers as bifunctional oxygen catalyst derived from a Prussian blue analogue, J. Alloy. Compd. 740 (2018) 743–753, https://doi.org/10.1016/j.jallcom.2018.01.019.
[191] H. Zhou, F. Fan, H. Yu, Y. Xu, C. Yuan, Y. Wang, Flower-like mesoporous carbon with cobalt sulfide nanocrystalline as efficient bifunctional electrocatalysts for Zn-Air batteries, ChemCatChem 14 (2022), e202101807, https://doi.org/10.1002/cctc.202101807.
[192] V. Parthiban, P.V. Sruthibhai, R.S. Menon, S.K. Panda, A.K. Sahu, *In situ* fabrication of cobalt sulfide-decorated N,S co-doped mesoporous carbon and its application as an electrocatalyst for efficient oxygen reduction reaction, New J. Chem. 46 (2022) 10700–10709, https://doi.org/10.1039/d2nj00403h.
[193] L. Wang, S. Huang, D. Zeng, P. Zhu, X. Zhao, S. Liu, S. Mesoporous, N-codoped carbon/Co_xS_y hybrid catalyst for efficient bifunctional oxygen electrocatalysis in rechargeable Zn-Air batteries, Energy Fuels 35 (2021) 19811–19817, https://doi.org/10.1021/acs.energyfuels.1c03069.
[194] J. Ding, S. Ji, H. Wang, B.G. Pollet, R. Wang, Mesoporous CoS/N-doped carbon as HER and ORR bifunctional electrocatalyst for water electrolyzers and zinc-air batteries, ChemCatChem 11 (2019) 1026–1032, https://doi.org/10.1002/cctc.201801618.
[195] C. Han, Q. Li, D. Wang, Q. Lu, Z. Xing, X. Yang, Cobalt sulfide nanowires core encapsulated by a N, S codoped graphitic carbon shell for efficient oxygen reduction reaction, Small 14 (2018), 1703642, https://doi.org/10.1002/smll.201703642.
[196] X. Hong, Y. Xu, R. Wang, P. Du, Z. Zhao, K. Huang, H. Tang, Y. Liu, M. Lei, H. Wu, Boosting the performance of nitrogen-doped mesoporous carbon oxygen electrode with ultrathin 2D iron/cobalt selenides, Adv. Mater. Interfaces 7 (2020), https://doi.org/10.1002/admi.202000740.
[197] J. Ding, S. Ji, H. Wang, V. Linkov, R. Wang, Mesoporous cobalt selenide/nitrogen-doped carbon hybrid as bifunctional electrocatalyst for hydrogen evolution and oxygen reduction reactions, J. Power Sources 423 (2019) 1–8, https://doi.org/10.1016/j.jpowsour.2019.03.051.
[198] H. Wang, X. Qiu, Z. Peng, W. Wang, J. Wang, T. Zhang, L. Jiang, H. Liu, Cobalt-gluconate-derived high-density cobalt sulfides nanocrystals encapsulated within nitrogen and sulfur dual-doped micro/mesoporous carbon spheres for efficient electrocatalysis of oxygen reduction, J. Colloid Interface Sci. 561 (2020) 829–837, https://doi.org/10.1016/j.jcis.2019.11.065.
[199] C. Liu, P. Zuo, Y. Jin, X. Zong, D. Li, Y. Xiong, Defect-enriched carbon nanofibers encapsulating NiCo oxide for efficient oxygen electrocatalysis and rechargeable Zn-air batteries, J. Power Sources 473 (2020), 228604, https://doi.org/10.1016/j.jpowsour.2020.228604.
[200] L. Yan, H. Wang, J. Shen, J. Ning, Y. Zhong, Y. Hu, Formation of mesoporous Co/CoS/Metal-N-C@S, N-codoped hairy carbon polyhedrons as an efficient trifunctional electrocatalyst for Zn-air batteries and water splitting, Chem. Eng. J. 403 (2021), 126385, https://doi.org/10.1016/j.cej.2020.126385.
[201] Z. Li, X. Wang, J. Liu, C. Gao, L. Jiang, Y. Lin, A. Meng, 3D honeycomb nanostructure comprised of mesoporous N-doped carbon nanosheets encapsulating isolated cobalt and vanadium nitride nanoparticles as a highly efficient electrocatalyst for the oxygen reduction reaction, ACS Sustain. Chem. Eng. 8 (2020) 3291–3301, https://doi.org/10.1021/acssuschemeng.9b06934.
[202] Y. Zhang, X. Wang, F. Luo, Y. Tan, L. Zeng, B. Fang, A. Liu, Rock salt type $NiCo_2O_3$ supported on ordered mesoporous carbon as a highly efficient electrocatalyst for oxygen evolution reaction, Appl. Catal. B Environ. 256 (2019), 117852, https://doi.org/10.1016/j.apcatb.2019.117852.
[203] T. Oh, D. Park, J. Kim, $CoFe_2O_4$ nanoparticles anchored on N/S co-doped mesoporous carbon spheres as efficient bifunctional electrocatalysts for oxygen catalytic reactions, Int. J. Hydrog. Energy 44 (2019) 2645–2655, https://doi.org/10.1016/j.ijhydene.2018.11.216.
[204] T. Oh, S. Ryu, H. Oh, J. Kim, $MnCo_2O_4$ nanoparticles supported on nitrogen and sulfur co-doped mesoporous carbon spheres as efficient electrocatalysts for oxygen catalytic reactions, Dalton Trans. 48 (2019) 945–953, https://doi.org/10.1039/c8dt03955k.
[205] K.J. Lee, D.Y. Shin, A. Byeon, A. Lim, Y.S. Jo, A. Begley, D.H. Lim, Y.E. Sung, H. S. Park, K.H. Chae, S.W. Nam, K.Y. Lee, J.Y. Kim, Hierarchical cobalt-nitride and -oxide co-doped porous carbon nanostructures for highly efficient and durable bifunctional oxygen reaction electrocatalysts, Nanoscale 9 (2017) 15846–15855, https://doi.org/10.1039/c7nr06646e.
[206] Z. Wang, S. Xiao, Y. An, X. Long, X. Zheng, X. Lu, Y. Tong, S. Yang, $Co(II)_{1-x}Co(0)_{x/3}Mn(III)_{2x/3}S$ nanoparticles supported on B/N-codoped mesoporous nanocarbon as a bifunctional electrocatalyst of oxygen reduction/evolution for high-performance zinc-air batteries, ACS Appl. Mater. Interfaces 8 (2016) 13348–13359, https://doi.org/10.1021/acsami.5b12803.
[207] M. Shen, C. Ruan, Y. Chen, C. Jiang, K. Ai, L. Lu, Covalent entrapment of cobalt-iron sulfides in N-doped mesoporous carbon: extraordinary bifunctional electrocatalysts for oxygen reduction and evolution reactions, ACS Appl. Mater. Interfaces 7 (2015) 1207–1218, https://doi.org/10.1021/am507033x.
[208] Z. Wu, T. Wang, J.J. Zou, Y. Li, C. Zhang, J.J. Zou, C. Zhang, Amorphous nickel oxides supported on carbon nanosheets as high-performance catalysts for electrochemical synthesis of hydrogen peroxide, ACS Catal. (2022) 5911–5920, https://doi.org/10.1021/acscatal.2c01829.
[209] X. Bo, Y. Zhang, M. Li, A. Nsabimana, L. Guo, $NiCo_2O_4$ spinel/ordered mesoporous carbons as noble-metal free electrocatalysts for oxygen reduction reaction and the influence of structure of catalyst support on the electrochemical activity of $NiCo_2O_4$, J. Power Sources 288 (2015) 1–8, https://doi.org/10.1016/j.jpowsour.2015.04.110.
[210] M.F. Qiao, Y. Wang, L. Li, G.Z. Hu, G.A. Zou, X. Mamat, Y.M. Dong, X. Hu, Self-templated nitrogen-doped mesoporous carbon decorated with double transition-metal active sites for enhanced oxygen electrode catalysis, Rare Met. 39 (2020) 824–833, https://doi.org/10.1007/s12598-019-01345-9.
[211] T. Zhang, Z. Li, Z. Zhang, L. Wang, P. Sun, S. Wang, Design of a three-dimensional interconnected hierarchical micro-mesoporous structure of graphene as support material for Spinel $NiCo_2O_4$ electrocatalysts toward oxygen reduction reaction, J. Phys. Chem. C 122 (2018) 27469–27476, https://doi.org/10.1021/acs.jpcc.8b08692.
[212] K. Wan, J. Luo, X. Zhang, C. Zhou, J.W. Seo, P. Subramanian, J.W. Yan, J. Fransaer, A template-directed bifunctional NiS: x/nitrogen-doped mesoporous carbon electrocatalyst for rechargeable Zn-air batteries, J. Mater. Chem. A 7 (2019) 19889–19897, https://doi.org/10.1039/c9ta06446j.
[213] X. Wu, S. Li, B. Wang, J. Liu, M. Yu, Mesoporous Ni-Co based nanowire arrays supported on three-dimensional N-doped carbon foams as non-noble catalysts for efficient oxygen reduction reaction, Microporous Mesoporous Mater. 231 (2016) 128–137, https://doi.org/10.1016/j.micromeso.2016.05.019.
[214] C. Si, Y. Zhang, C. Zhang, H. Gao, W. Ma, L. Lv, Z. Zhang, Mesoporous nanostructured spinel-type MFe_2O_4 (M = Co, Mn, Ni) oxides as efficient bi-functional electrocatalysts towards oxygen reduction and oxygen evolution, Electrochim. Acta 245 (2017) 829–838, https://doi.org/10.1016/j.electacta.2017.06.029.
[215] X. Zhao, Y. Liu, Origin of selective production of hydrogen peroxide by electrochemical oxygen reduction, J. Am. Chem. Soc. 143 (2021) 9423–9428, https://doi.org/10.1021/jacs.1c02186.
[216] L. Roldán, L. Truong-Phuoc, A. Ansón-Casaos, C. Pham-Huu, E. García-Bordejé, Mesoporous carbon doped with N,S heteroatoms prepared by one-pot auto-assembly of molecular precursor for electrocatalytic hydrogen peroxide synthesis, Catal. Today 301 (2018) 2–10, https://doi.org/10.1016/j.cattod.2016.12.020.
[217] L. Jing, Q. Tian, P. Su, H. Li, Y. Zheng, C. Tang, J. Liu, Mesoporous Co-O-C nanosheets for electrochemical production of hydrogen peroxide in acidic medium, J. Mater. Chem. A 10 (2022) 4068–4075, https://doi.org/10.1039/d1ta10416k.

[218] H. Xu, S. Zhang, J. Geng, G. Wang, H. Zhang, Cobalt single atom catalysts for the efficient electrosynthesis of hydrogen peroxide, Inorg. Chem. Front. 8 (2021) 2829–2834, https://doi.org/10.1039/d1qi00158b.
[219] Y. Tan, C. Xu, G. Chen, X. Fang, N. Zheng, Q. Xie, Facile synthesis of manganese-oxide-containing mesoporous nitrogen-doped carbon for efficient oxygen reduction, Adv. Funct. Mater. 22 (2012) 4584–4591, https://doi.org/10.1002/adfm.201201244.
[220] J. Mao, P. Liu, J. Li, J. Yan, S. Ye, W. Song, Accelerated intermediate conversion through nickel doping into mesoporous Co-N/C nanopolyhedron for efficient ORR, J. Energy Chem. 73 (2022) 240–247, https://doi.org/10.1016/j.jechem.2022.04.047.
[221] Y. Sun, I. Sinev, W. Ju, A. Bergmann, S. Dresp, S. Kühl, C. Spöri, H. Schmies, H. Wang, D. Bernsmeier, B. Paul, R. Schmack, R. Kraehnert, B. Roldan Cuenya, P. Strasser, Efficient electrochemical hydrogen peroxide production from molecular oxygen on nitrogen-doped mesoporous carbon catalysts, ACS Catal. 8 (2018) 2844–2856, https://doi.org/10.1021/acscatal.7b03464.
[222] V. Perazzolo, C. Durante, A. Gennaro, Nitrogen and sulfur doped mesoporous carbon cathodes for water treatment, J. Electroanal. Chem. 782 (2016) 264–269, https://doi.org/10.1016/j.jelechem.2016.10.037.
[223] V. Duraisamy, S.M. Senthil Kumar, N and P dual heteroatom doped mesoporous hollow carbon as an efficient oxygen reduction reaction catalyst in alkaline electrolyte, Int. J. Hydrog. Energy 47 (2022) 17992–18006, https://doi.org/10.1016/j.ijhydene.2022.03.284.
[224] V. Duraisamy, R. Krishnan, S.M.S. Kumar, Architecture of large surface area N-doped mesoporous carbon sheets as sustainable electrocatalyst for oxygen reduction reaction in alkaline electrolyte, Mater. Res. Bull. 149 (2022), https://doi.org/10.1016/j.materresbull.2022.111729.
[225] C. Deng, L. Pan, F. Ji, W. Du, J. Zhang, Y. Sun, H. Zhong, Hybrid dual-template induced nitrogen-doped hierarchically porous carbon as highly efficient oxygen reduction electrocatalyst, Int. J. Hydrog. Energy 46 (2021) 36167–36175, https://doi.org/10.1016/j.ijhydene.2021.08.156.
[226] Y. Niu, X. Huang, W. Hu, Fe_3C nanoparticle decorated Fe/N doped graphene for efficient oxygen reduction reaction electrocatalysis, J. Power Sources 332 (2016) 305–311, https://doi.org/10.1016/j.jpowsour.2016.09.130.
[227] A. Kong, Y. Kong, X. Zhu, Z. Han, Y. Shan, Ordered mesoporous Fe (or Co)-N-graphitic carbons as excellent non-precious-metal electrocatalysts for oxygen reduction, Carbon 78 (2014) 49–59, https://doi.org/10.1016/j.carbon.2014.06.047. N. Y.
[228] Y.L. Liu, E.Y. Xu, P.C. Sun, T.H. Chen, N-doped porous carbon nanosheets with embedded iron carbide nanoparticles for oxygen reduction reaction in acidic media, Int. J. Hydrog. Energy 40 (2015) 4531–4539, https://doi.org/10.1016/j.ijhydene.2015.02.018.
[229] D. Guo, S. Han, R. Ma, Y. Zhou, Q. Liu, J. Wang, Y. Zhu, *In situ* formation of iron-cobalt sulfides embedded in N,S-doped mesoporous carbon as efficient electrocatalysts for oxygen reduction reaction, Microporous Mesoporous Mater. 270 (2018) 1–9, https://doi.org/10.1016/j.micromeso.2018.04.044.
[230] C. Li, C. He, F. Sun, M. Wang, J. Wang, Y. Lin, Incorporation of Fe_3C and pyridinic N Active Sites with a moderate N/C ratio in Fe-N mesoporous carbon materials for enhanced oxygen reduction reaction activity, ACS Appl. Nano Mater. 1 (2018) 1801–1810, https://doi.org/10.1021/acsanm.8b00235.
[231] S.H. Lee, J. Kim, D.Y. Chung, J.M. Yoo, H.S. Lee, M.J. Kim, B.S. Mun, S.G. Kwon, Y.E. Sung, T. Hyeon, Design principle of Fe-N-C electrocatalysts: how to optimize multimodal porous structures? J. Am. Chem. Soc. 141 (2019) 2035–2045, https://doi.org/10.1021/jacs.8b11129.
[232] Z. Mo, W. Yang, S. Gao, J.K. Shang, Y. Ding, W. Sun, Q. Li, Efficient oxygen reduction reaction by a highly porous, nitrogen-doped carbon sphere electrocatalyst through space confinement effect in nanopores, J. Adv. Ceram. 10 (2021) 714–728, https://doi.org/10.1007/s40145-021-0466-1.